



ELSEVIER

doi:10.1016/j.gca.2005.03.050

Oxygen, magnesium and chromium isotopic ratios of presolar spinel grains

ERNST ZINNER,^{1,*} LARRY R. NITTLER,² PETER HOPPE,³ ROBERTO GALLINO,^{4,5} OSCAR STRANIERO⁶ and CONEL M. O'D. ALEXANDER²¹Laboratory for Space Sciences and the Physics Department, Washington University, One Brookings Drive, St. Louis, MO 63130, USA²Department of Terrestrial Magnetism, Carnegie Institution of Washington, 5241 Broad Branch Road, NW Washington DC, 20015, USA³Max-Planck-Institut für Chemie, Kosmochemie, P.O. Box 3060, D-55020 Mainz, Germany⁴Dipartimento di Fisica Generale, Università di Torino, Via P. Giuria 1, I-10125 Torino, Italy⁵Centre for Stellar and Planetary Astrophysics, School of Mathematical Sciences, Monash University, Victoria 3800 Australia⁶INAF, Osservatorio Astronomico di Teramo, Italy

(Received May 13, 2004; accepted in revised form March 28, 2005)

Abstract—Oxygen isotopic measurements of 20 spinel (MgAl_2O_4) grains from the CM2 meteorite Murray (average diameter $0.45 \mu\text{m}$), seven spinel grains from ordinary chondrites (OC, 0.3 to $2 \mu\text{m}$) and three spinel grains from the CI chondrite Orgueil (0.4 to $0.7 \mu\text{m}$) have revealed large anomalies and thus established their presolar origin. Their O isotopic ratios fall into all four previously defined groups and indicate that most of the grains come from red giant branch (RGB) or asymptotic giant branch (AGB) stars. With the NanoSIMS, we measured the magnesium isotopic compositions of all 30 grains. We also measured the Cr isotopic ratios of the three Orgueil grains and one OC grain. Two of the Orgueil grains are very rich in Cr, with a composition representing a 1:1 solid solution of spinel and magnesiochromite (MgCr_2O_4). At least 13 of the 30 analyzed grains have substantial Mg isotopic anomalies. They have excesses in ^{26}Mg , primarily from the decay of ^{26}Al , as well as excesses and deficits in ^{25}Mg . We present the results of new model calculations of the evolution of Mg and Al isotopic ratios in the envelopes of AGB stars for a range of masses (1.5 , 2 , 3 , and $5 M_{\odot}$), metallicities ($1/6$, $1/3$, $1/2$ and $1Z_{\odot}$) and different prescriptions for mass loss by stellar winds. Comparisons of the grain data with these models show that inferred $^{26}\text{Al}/^{27}\text{Al}$ ratios of several grains are much larger than predicted and require an extra production process for ^{26}Al , most likely the result of deep mixing in the star's envelope, also called cool bottom processing (CBP). One grain is probably from an intermediate-mass ($\sim 5 M_{\odot}$) AGB star in which the envelope extended down to the H-burning shell ("hot bottom burning"). On average, $^{26}\text{Al}/^{27}\text{Al}$ ratios in oxide grains are larger than those in SiC grains from AGB stars (mainstream, Y and Z grains), whose $^{26}\text{Al}/^{27}\text{Al}$ ratios agree with AGB models. This indicates that the parent stars of oxide grains with high ($> 5 \times 10^{-3}$) $^{26}\text{Al}/^{27}\text{Al}$ ratios are fundamentally different from those of SiC grains. The CBP experienced by the former might have prevented these stars from becoming the carbon stars that would have produced presolar SiC grains. Copyright © 2005 Elsevier Ltd

1. INTRODUCTION

Silicon carbide is the most studied presolar grain type (Nittler, 2003; Zinner, 2003). One reason for this is that essentially all SiC grains in primitive meteorites are of presolar origin and that, because of its chemically refractory nature, almost pure separates of SiC can be isolated from meteorites. Another reason is that SiC contains relatively high concentrations of trace elements that can be analyzed for their isotopic compositions in addition to the major elements C and Si. The situation is not as simple for oxygen-rich presolar grains because solar system material is dominated by O-rich phases and O-rich presolar grains have to be identified amongst much more abundant solar-system grains by isotopic analysis (usually of O) of single grains. The early studies of presolar oxide grains have concentrated on corundum grains because the proportion of presolar corundum grains among all corundum grains seems to be higher than that of other oxides, at least for grains $> 1 \mu\text{m}$, and residues rich in corundum grains can be produced by chemical separation of primitive meteorites (Nittler et al., 1997; Choi et al., 1998, 1999). In contrast, presolar spinel was believed to be quite rare (Nittler et al., 1997; Choi et al., 1998; Krestina et al., 2002).

This situation changed with the advent of the NanoSIMS, which makes the isotopic analysis of sub- μm grains possible (Slodzian et al., 2003). It was found that the abundance of presolar grains among spinel grains from primitive meteorites increases with decreasing grain size and as of today more than 250 presolar spinel grains have been identified, albeit most of them in tightly packed grain deposits (Nguyen et al., 2003; Zinner et al., 2003). The availability of presolar spinel grains presents the opportunity to measure their Mg isotopic ratios with relatively high precision, since Mg is a major constituent of the grains. Magnesium isotopic ratios of a large number of SiC, graphite and corundum grains have previously been measured (Nittler et al., 1997; Huss et al., 1997; Choi et al., 1998, 1999; Zinner, 2003). However, because of the low Mg concentrations in these grains their analysis mostly detected radiogenic ^{26}Mg from the decay of extinct ^{26}Al ($\tau_{1/2} = 7.1 \times 10^5 \text{ yr}$) and thus served for the determination of initial $^{26}\text{Al}/^{27}\text{Al}$ ratios. Information on the $^{25}\text{Mg}/^{24}\text{Mg}$ ratios has been more limited, due to large error bars and the possibility of terrestrial contamination.

Here we present Mg measurements on 20 Al-Mg spinel grains from the CM2 carbonaceous chondrite Murray, on one Al-Mg and two Cr-rich spinels from the CI carbonaceous chondrite Orgueil, and on seven Al-Mg spinels from unequilibrated ordinary chondrites (OCs). We also report Cr isotopic

* Author to whom correspondence should be addressed (ekz@wustl.edu).

measurements of the three Orgueil grains and one OC grain. All grains have been determined to be of presolar origin on the basis of their O isotopic compositions. Preliminary results of this study have been reported by Nittler et al. (2003); Nittler and Alexander (2003b) and Zinner et al. (2004).

2. EXPERIMENTAL

The analyzed spinel grains from Murray were all from the spinel-rich separate CG (average grain size $0.45\ \mu\text{m}$) (Tang and Anders, 1988). Seven of them had their O isotopic ratios reported previously by Zinner et al. (2003) who analyzed 753 grains and found 9 presolar spinels. Oxygen isotopic analysis of another 500 CG grains with the Washington University NanoSIMS ion microprobe yielded an additional 13 presolar spinel grains. The analysis technique used has been described by Zinner et al. (2003). The seven spinel grains from ordinary chondrites are from a mixed acid-resistant residue of the OCs Semarkona (LL3.0), Bishunpur (LL3.1) and Krymka (LL3.1), prepared using methods similar to those for the Murray residue. These grains ranged in size from 0.3 to $2\ \mu\text{m}$ and were identified as presolar by automated O isotopic analysis of all three O isotopes in the Carnegie ims-6f ion microprobe (Nittler and Alexander, 1999, 2003a). One Al-Mg spinel and two Cr-rich oxide grains were found in a residue from the Orgueil carbonaceous chondrite (CI) by the same method. The residue was prepared by first dissolving a small sample of the meteorite in a mixture of CsF and HF. An aliquot of the resulting organic-rich residue was ashed in an oxygen plasma to destroy the organic matter and a $1\text{--}5\ \mu\text{m}$ size separate of the remaining material was deposited on ion probe mounts for the automated analyses. The presolar grains analyzed in this study ranged from 0.4 to $0.7\ \mu\text{m}$ in diameter.

Magnesium isotopic ratios of the OC and Orgueil grains and of 7 Murray grains were determined with the NanoSIMS ion microprobe at the Max-Planck-Institute for Chemistry in Mainz, those of the remaining 13 Murray grains with the NanoSIMS at Washington University in St. Louis. A primary O^- beam of $\sim 10\ \text{pA}$ and $0.2\text{--}0.3\ \mu\text{m}$ diameter was rastered over $2 \times 2\ \mu\text{m}^2$ areas (for the OC and Orgueil grains) or $0.4 \times 0.4\ \mu\text{m}^2$ areas (for the Murray grains) centered on the selected grains. Positive secondary ions of the three Mg isotopes and of ^{27}Al were measured in multi-detection mode with four different electron multipliers (EMs). Other spinel grains on the same sample mounts, whose O isotopic ratios were normal and which were thus assumed to be of solar-system origin, were also measured as Mg isotopic “standards.” The Mg isotopic ratios and the Al/Mg ratios of the presolar grains were determined by comparison with these grains. The reproducibility of $^{25}\text{Mg}/^{24}\text{Mg}$ and $^{26}\text{Mg}/^{24}\text{Mg}$ ratios on different “standard” grains was within several permil. These variations are included in the errors given for $\delta^{25}\text{Mg}/^{24}\text{Mg}$ and $\delta^{26}\text{Mg}/^{24}\text{Mg}$ in Table 1. The relative Al^+/Mg^+ sensitivity factor was calculated under the assumption that the spinel grains of solar-system origin have atomic $\text{Al}/\text{Mg} = 2$. This resulted in relative Al^+/Mg^+ sensitivity factors of between 1.43 and 2.04 (error of $\sim 15\%$ each), depending on the measurement session.

Chromium isotopes were measured in four grains with the Mainz NanoSIMS in a combined peak-jumping/multi-detection mode. The magnet was cycled through three field settings. In the first, $^{27}\text{Al}^+$ was measured on one EM, in the second, $^{47}\text{Ti}^+$, $^{50}\text{Cr}^+$, $^{52}\text{Cr}^+$, $^{54}\text{Cr}^+$ and $^{56}\text{Fe}^+$ were simultaneously detected on five EMs, and in the third $^{48}\text{Ti}^+$, $^{53}\text{Cr}^+$ and $^{57}\text{Fe}^+$ were measured on three EMs. The Ti and Fe isotopes were measured to correct for isobaric interferences of ^{50}Ti on ^{50}Cr and ^{54}Fe on ^{54}Cr . For these corrections we assumed normal Ti and Fe isotopic ratios. We obtained uncertainties for the corrections by taking the maximum isotopic anomalies in ^{50}Ti observed in mainstream SiC grains (Hoppe et al., 1994; Alexander and Nittler, 1999) and the uncertainties in $^{54}\text{Fe}/^{56}\text{Fe}$ ratios in SiC grains (Marhas et al., 2004) into account. These uncertainties were included in the uncertainties of the final Cr isotopic ratios. Other Cr-rich oxide grains on the sample mounts were used as isotopic standards; these indicate a one-sigma measurement reproducibility of 8‰, 4‰, 9‰, and 16‰ for $^{50}\text{Cr}/^{52}\text{Cr}$, $^{53}\text{Cr}/^{52}\text{Cr}$, $^{54}\text{Cr}/^{52}\text{Cr}$, and $^{57}\text{Fe}/^{56}\text{Fe}$, respectively.

3. RESULTS

The O and Mg isotopic ratios of the measured grains are given in Table 1 and are plotted in Figures 1 and 2. Grains from Murray, the OCs, and Orgueil are given the prefixes M, OC and OR, respectively. According to their O isotopic ratios, the spinel grains fall into all of the four groups, indicated in Figure 1, that were previously defined for corundum grains (Nittler et al., 1997). While 17 grains cluster around normal Mg isotopic ratios (both $\delta^{25}\text{Mg}/^{24}\text{Mg}$ and $\delta^{26}\text{Mg}/^{24}\text{Mg}$ are $< 20\ \text{‰}$), the remaining 13 grains have substantial Mg anomalies (Fig. 2). The most extreme composition with ^{25}Mg and ^{26}Mg excesses of 430‰ and 1170‰, respectively, is exhibited by the grain OC2, which also has the most extreme O isotopic ratios (Fig. 1). The grains M16, M20, OR4 and OC15 also have excesses in both heavy Mg isotopes. In contrast, the three grains M12, M17 and M18 have ^{25}Mg depletions and ^{26}Mg excesses. Four Murray grains and one OC grain have ^{26}Mg excesses, but their $^{25}\text{Mg}/^{24}\text{Mg}$ ratios are normal within 2σ errors.

The chromium isotopic ratios of the four measured grains are given in Table 2. The $^{57}\text{Fe}/^{56}\text{Fe}$ ratios for these grains are solar within large ($> 10\%$) errors. Two grains, OR1 and OR4 have moderate, yet significant ^{54}Cr depletions of $\sim 10\%$, relative to solar. All other measured Cr ratios are solar within analytical uncertainties.

There are some variations in the Al/Mg ratios of the spinel grains, indicating that they are not strictly stoichiometric in their elemental compositions (Table 1). Higher-than-stoichiometric Al/Mg ratios have previously been observed in CAIs and have been interpreted to indicate extremely high temperatures (Simon et al., 1994). It is quite possible that during decreasing temperatures in the outflowing stellar envelope corundum, which is predicted to condense at higher temperature (Wood and Hashimoto, 1993), was replaced by spinel of non-stoichiometric composition. The low Al/Mg ratios observed in some grains are more puzzling. Based on Ti^+/Al^+ and Cr^+/Al^+ secondary ion ratios for the OC and Orgueil spinel grains, we estimate Ti contents in the range of 120–680 ppm wt and Cr contents in the range of 0.2 to 2.7% wt. However, these concentrations are too low to explain Al/Mg ratios of ~ 1.5 seen in three grains (Table 1).

4. DISCUSSION

Before the present study, only two presolar spinel grains, T3 from Tieschitz (Nittler et al., 1994) and S-S21 from Semarkona (Choi et al., 1998), had their Mg isotopic compositions measured. Our new data provide the opportunity to compare the O and Mg isotopic compositions of a larger sample of spinel grains. With the exception of the group 4 grains M13 and M17, the grains studied here belong to groups 1, 2 and 3 according to their O isotopic ratios and most likely have an origin in red giant branch (RGB) or asymptotic giant branch (AGB) stars (Nittler et al., 1997). Group 1 grains are believed to come from stars with close-to-solar metallicity, group 2 grains from stars that experienced CBP (Wasserburg et al., 1995), group 3 grains from stars of low metallicity. The origin of group 4 grains is more uncertain; proposed stellar sources include (1) AGB stars of higher-than solar metallicity (Nittler et al., 1997); (2) AGB stars in which ^{18}O produced by He burning of ^{14}N during early thermal pulses was mixed into the envelope during third

Table 1. Oxygen and magnesium isotopic ratios, inferred $^{26}\text{Al}/^{27}\text{Al}$ ratios and inferred initial parent star masses of presolar spinel grains.

Grain	$^{17}\text{O}/^{16}\text{O} \pm 1\sigma$	$^{18}\text{O}/^{16}\text{O} \pm 1\sigma$	$\delta^{25}\text{Mg}/^{24}\text{Mg} \pm 1\sigma$	$\delta^{26}\text{Mg}/^{24}\text{Mg} \pm 1\sigma$	$\text{Al}/\text{Mg}^{\&} \pm 1\sigma$	$^{26}\text{Al}/^{27}\text{Al}^{\text{s}} \pm 1\sigma$	Mass M_{\odot}
Solar	3.830×10^{-4}	2.0052×10^{-3}	0.12663*	0.13932*			
OCs							
OC1	$8.93 \pm .91 \times 10^{-4}$	$7.96 \pm 1.92 \times 10^{-4}$	-2.0 ± 5.0	8.0 ± 8.0	2.52 ± 0.45	$<4 \times 10^{-4}$	
OC2	$1.25 \pm .07 \times 10^{-3}$	$6.94 \pm 1.34 \times 10^{-5}$	433.0 ± 10.0	1170.0 ± 15.0	2.18 ± 0.39	$4.0 \pm .8 \times 10^{-2}$	
OC3	$1.06 \pm .05 \times 10^{-3}$	$1.85 \pm .06 \times 10^{-3}$	4.0 ± 9.0	29.0 ± 11.0	2.39 ± 0.43	$1.2 \pm .6 \times 10^{-3}$	1.66
OC7	$3.57 \pm .07 \times 10^{-4}$	$1.66 \pm .06 \times 10^{-3}$	-7.0 ± 4.0	-8.0 ± 7.0	2.18 ± 0.39		1.10
OC10	$3.49 \pm .07 \times 10^{-4}$	$1.59 \pm .05 \times 10^{-3}$	-5.0 ± 4.0	-6.0 ± 7.0	2.08 ± 0.37		1.12
OC11	$4.78 \pm .12 \times 10^{-4}$	$1.77 \pm .06 \times 10^{-3}$	2.0 ± 5.0	-6.0 ± 7.0	1.54 ± 0.28		1.29
OC15	$4.02 \pm .14 \times 10^{-4}$	$1.70 \pm .08 \times 10^{-3}$	21.0 ± 7.0	23.0 ± 9.0	1.91 ± 0.34	$<1 \times 10^{-3}$	1.20
Orgueil							
OR1	$1.20 \pm .12 \times 10^{-3}$	$1.97 \pm .78 \times 10^{-4}$	46.0 ± 37.0	-26.0 ± 33.0	1.58 ± 0.24		
OR2	$1.09 \pm .07 \times 10^{-3}$	$1.61 \pm .13 \times 10^{-3}$	-17.0 ± 9.0	-13.0 ± 8.0	1.44 ± 0.24		1.67
OR4	$1.06 \pm .11 \times 10^{-3}$	$6.76 \pm 1.30 \times 10^{-4}$	40.0 ± 9.0	60.0 ± 8.0	2.00 ± 0.24	$2.1 \pm .5 \times 10^{-4}$	
Murray							
M1	$5.08 \pm .14 \times 10^{-4}$	$1.76 \pm .03 \times 10^{-3}$	5.5 ± 6.5	78.7 ± 6.8	3.00 ± 0.47	$2.7 \pm .5 \times 10^{-3}$	1.34
M2	$7.64 \pm .19 \times 10^{-4}$	$1.93 \pm .03 \times 10^{-3}$	-10.6 ± 5.5	11.4 ± 4.5	2.90 ± 0.46	$8.1 \pm 2.2 \times 10^{-4}$	1.50
M3	$4.13 \pm .12 \times 10^{-4}$	$1.82 \pm .03 \times 10^{-3}$	-2.2 ± 5.8	9.3 ± 5.1	2.40 ± 0.37	$<4.8 \times 10^{-4}$	1.17
M4	$4.28 \pm .11 \times 10^{-4}$	$1.72 \pm .03 \times 10^{-3}$	-3.7 ± 6.0	56.5 ± 4.3	1.90 ± 0.29	$3.3 \pm .6 \times 10^{-3}$	1.24
M5	$4.52 \pm .11 \times 10^{-4}$	$1.85 \pm .03 \times 10^{-3}$	0.9 ± 6.1	2.4 ± 4.8	2.20 ± 0.34	$<5.6 \times 10^{-4}$	1.23
M6	$4.76 \pm .10 \times 10^{-4}$	$1.75 \pm .02 \times 10^{-3}$	1.7 ± 3.7	12.8 ± 4.1	1.80 ± 0.29	$7.1 \pm 2.9 \times 10^{-4}$	1.30
M7	$6.49 \pm .14 \times 10^{-4}$	$1.84 \pm .02 \times 10^{-3}$	10.9 ± 4.5	12.1 ± 3.7	2.50 ± 0.39	$<4.0 \times 10^{-4}$	1.43
M8	$5.14 \pm .16 \times 10^{-4}$	$1.80 \pm .03 \times 10^{-3}$	-0.6 ± 6.1	-5.2 ± 5.6	1.90 ± 0.30		1.34
M9	$8.31 \pm .23 \times 10^{-4}$	$3.02 \pm 1.2 \times 10^{-4}$	13.2 ± 8.8	9.3 ± 7.5	2.10 ± 0.32	$<8.0 \times 10^{-4}$	
M10	$3.10 \pm .06 \times 10^{-4}$	$1.71 \pm .02 \times 10^{-3}$	-12.9 ± 5.6	3.8 ± 4.8	2.10 ± 0.33	$8.6 \pm 3.0 \times 10^{-4}$	0.81
M11	$4.10 \pm .08 \times 10^{-4}$	$1.77 \pm .02 \times 10^{-3}$	2.4 ± 7.6	1.0 ± 5.5	1.90 ± 0.30		1.19
M12	$1.22 \pm .04 \times 10^{-3}$	$1.78 \pm .11 \times 10^{-4}$	-51.2 ± 7.2	351.3 ± 7.0	2.20 ± 0.34	$1.9 \pm .3 \times 10^{-2}$	
M13	$5.09 \pm .10 \times 10^{-4}$	$2.82 \pm .03 \times 10^{-3}$	-10.6 ± 6.6	44.7 ± 5.6	1.80 ± 0.28	$3.2 \pm .6 \times 10^{-3}$	
M14	$7.28 \pm .32 \times 10^{-4}$	$1.94 \pm .07 \times 10^{-3}$	-0.9 ± 13.3	7.3 ± 14.0	2.80 ± 0.30	$<1 \times 10^{-3}$	1.47
M15	$4.29 \pm .15 \times 10^{-4}$	$1.77 \pm .05 \times 10^{-3}$	-2.6 ± 3.9	49.3 ± 7.6	2.16 ± 0.32	$2.5 \pm .6 \times 10^{-3}$	1.22
M16	$7.82 \pm .22 \times 10^{-4}$	$1.02 \pm .02 \times 10^{-3}$	146.4 ± 4.3	491.7 ± 8.0	2.28 ± 0.33	$1.9 \pm .3 \times 10^{-2}$	1.55
M17	$5.60 \pm .17 \times 10^{-4}$	$2.62 \pm .05 \times 10^{-3}$	-64.1 ± 4.6	137.1 ± 8.1	2.12 ± 0.30	$1.0 \pm 0.2 \times 10^{-2}$	
M18	$8.14 \pm .26 \times 10^{-4}$	$1.17 \pm .03 \times 10^{-3}$	-71.9 ± 5.1	228.4 ± 8.6	2.59 ± 0.34	$1.2 \pm .2 \times 10^{-2}$	1.56
M19	$7.09 \pm .29 \times 10^{-4}$	$1.83 \pm .05 \times 10^{-3}$	6.9 ± 7.3	9.4 ± 9.5	2.21 ± 0.28	$<9 \times 10^{-4}$	1.47
M20	$7.15 \pm .26 \times 10^{-4}$	$1.30 \pm .04 \times 10^{-3}$	63.4 ± 5.2	176.5 ± 10.6	2.58 ± 0.30	$5.9 \pm .8 \times 10^{-3}$	1.51

* $^{25}\text{Mg}/^{24}\text{Mg}$ and $^{26}\text{Mg}/^{24}\text{Mg}$ ratios.

& Atomic ratio.

^s The inferred $^{26}\text{Al}/^{27}\text{Al}$ ratios were calculated by extrapolating the measured data points back to a slope-1.95 (for $\delta^{25}\text{Mg} > 0$) and a slope-one line (for $\delta^{25}\text{Mg} < 0$) in a δ -value 3-isotope plot (see Figs. 4a,b). For details see text. An exception is grains OC2 where the data point was extrapolated back to the evolution line predicted for AGB nucleosynthesis in a $5M_{\odot}$ star (Fig. 4b).

dredge-up (TDU) (Boothroyd and Sackmann, 1988); and (3) supernovae (Choi et al., 1998).

The O and Mg isotopic compositions of the spinel grains, in principle, provide important information about the chemical evolution of the Galaxy because they are influenced by the initial compositions of the parent stars. They provide also information about stellar nucleosynthesis occurring at different evolutionary stages of the stars. The likely parent stars of the grains, inferred from their O isotopic ratios, AGB stars, are low-to-medium mass ($1.5\text{--}6 M_{\odot}$) stars in the last stage of their evolution. After exhaustion of H in their center during the main sequence phase and exhaustion of He during the red giant phase they consist of a C-O core (that will become a White Dwarf after the star will have lost its envelope) and a convective envelope. Nuclear burning takes place alternately in two thin shells, the He- and H-burning shell. After each short He-burning event (the thermal pulse), the convective envelope dips down into regions where nuclear burning had taken place and in the so-called third dredge-up (TDU) mixes freshly synthe-

sized material to the star's surface. For more details we refer the reader to the review by Busso et al. (1999).

In the following sections we will discuss the O and Mg isotopic ratios of the spinel grains within the framework of an AGB-star origin of these grains. We first describe in some detail the nuclear reactions that are responsible for the O and Mg isotopic ratios expected to be found in the envelope of such stars (section 4.1). The O isotopic ratios found in O-rich grains believed to have a RGB or AGB star origin have been discussed in detail before (Nittler et al., 1997; Choi et al., 1998, 1999). They can be used to infer the mass and metallicity of the grains' parent stars. Next we present detailed theoretical models on the evolution of the Mg isotopic abundances and the $^{26}\text{Al}/^{27}\text{Al}$ ratios in the envelope of AGB stars (section 4.2). A comparison with the grain data (section 4.3) shows that the standard models cannot reproduce the Mg isotopic compositions of all grains and additional processes have to be considered. Two of these, hot bottom burning and cool bottom processing, are discussed in more detail in section 4.4. As already

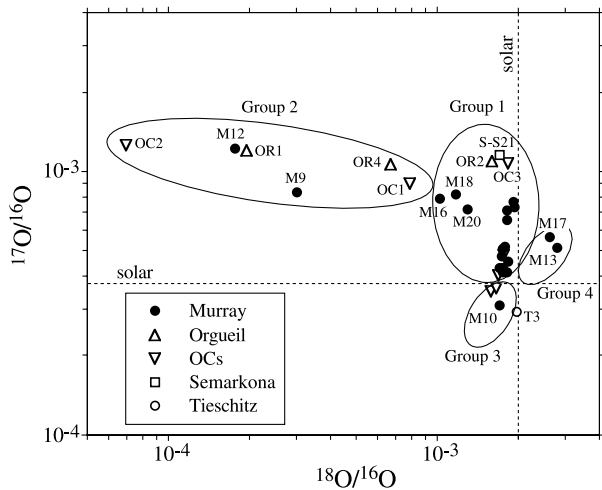


Fig. 1. Oxygen isotopic ratios of presolar spinel grains in which Mg isotopic ratios were determined. Included is grain T3 from Tieschitz reported by Nittler et al. (1994) and S-S21 from Semarkona reported by Choi et al. (1998). Also shown are the four groups identified for presolar corundum grains by Nittler et al. (1997).

mentioned, galactic chemical evolution affects the isotopic compositions of the grains through the initial compositions of their parent stars and we consider this question for the Mg isotopic ratios of the spinel grains (section 4.5). One puzzling observation is that inferred $^{26}\text{Al}/^{27}\text{Al}$ ratios in oxide grains are, on average, substantially larger than those in SiC grains and we discuss possible reasons for this difference (section 4.6). Finally, we include a short discussion of the Cr isotopic ratios measured in four grains (Section 4.7).

4.1. Nuclear Reactions Affecting the O and Mg Isotopes

There is no obvious correlation between the isotopic ratios of the O and Mg in the spinel grains. Let us first consider the grains from group 2. Grains M12 and OR1 have almost identical O isotopic ratios, but very different Mg isotopic ratios, with M12 having a ^{25}Mg depletion and large ^{26}Mg excess while OR1 has normal Mg isotopic ratios within experimental uncertainty. Also, M9 and OC1 have close-to-normal Mg isotopic ratios, whereas OR4 has moderate and OC2 extreme excesses in the two heavy Mg isotopes. Likewise, M16 and M18, both Group-1 grains, have similar O isotopic ratios, but have ^{25}Mg excesses and deficits, respectively. Conversely, the grains M12, M17, and M18, which have pronounced ^{25}Mg depletions and ^{26}Mg excesses, belong to groups 2, 4, and 1 according to their O isotopic ratios.

However, a correlation between the O and Mg isotopic ratios in individual grains is not necessarily to be expected because different nucleosynthetic processes taking place at different stages of stellar evolution affect the isotopic abundances of these two elements.

4.1.1. Oxygen isotopes

If we assume an RGB or AGB origin for the grains, their O isotopic compositions are first determined by the original compositions of their parent stars. According to galactic chemical

evolution (GCE) models, the ratios of the secondary¹ isotopes ^{17}O and ^{18}O relative to the primary¹ isotope ^{16}O are expected to increase during the evolution of the Galaxy and thus as function of stellar metallicity (Timmes et al., 1995). These original ratios are modified by H burning in deep hot layers during the main-sequence phase of low-to-intermediate mass stars. Material from these layers is subsequently mixed into the envelope during the first (and second) dredge-up (Boothroyd et al., 1994; Boothroyd and Sackmann, 1999). While the TDU in thermally-pulsing (TP) AGB stars does not have any significant effect on the O isotopic composition of the envelope, hot bottom burning (HBB) and cool bottom processing (CBP) can. HBB, predicted for AGB stars of larger than $\sim 4\text{--}5M_{\odot}$, preferentially those of low metallicity (Boothroyd et al., 1995; Lattanzio et al., 1996, 1997), occurs when the convective envelope reaches into the top layers of the H-burning shell. This leads to almost complete destruction of ^{18}O and large excesses in ^{17}O (Boothroyd et al., 1995; Forestini and Charbonnel, 1997). However, the predicted $^{17}\text{O}/^{16}\text{O}$ ratios are typically higher than those observed in the ^{18}O -depleted (group 2) presolar oxide grains and HBB also cannot explain the range of $^{18}\text{O}/^{16}\text{O}$ ratios observed in these grains (Boothroyd et al., 1995). CBP is the name given to an extra mixing process postulated to occur in low-mass RGB and TP-AGB stars to explain the low $^{12}\text{C}/^{13}\text{C}$ ratios in RGB stars and the ^{18}O depletions of group 2 presolar oxide grains (Charbonnel, 1995; Wasserburg et al., 1995; Nollett et al., 2003). In this process, material is circulated from the convective envelope through hot regions of the underlying radiative zone close to the H-burning shell. The O isotopic ratios of presolar oxide grains have previously been discussed in considerable detail (Nittler et al., 1997; Choi et al., 1998, 1999; Nollett et al., 2003) and we do not want to repeat these discussions.

4.1.2. Magnesium and aluminum isotopes

GCE models indicate that the secondary isotopes ^{25}Mg and ^{26}Mg increase relative to the primary isotope ^{24}Mg as function of metallicity (Timmes et al., 1995; Goswami and Prantzos, 2000; Alibés et al., 2001; Fenner et al., 2003) and Huss et al. (1995) first interpreted the ^{25}Mg excess and the Ti isotopic ratios in a corundum grain from Orgueil in terms of GCE. Thus, as is the case for the O isotopes, the Mg isotopic ratios found in the envelope of RGB and AGB stars are determined by the initial ratios at the birth of the stars and are changed by nucleosynthetic processes during subsequent evolutionary stages.

During the main sequence phase, temperatures in the zones mixed to the surface by the first dredge-up are not high enough to cause any nuclear reactions involving the Mg isotopes; this is in contrast to the O isotopes. During the second dredge-up, which occurs in stars with $>3.5\text{--}4M_{\odot}$, ^{26}Al can be brought to the surface because the convective envelope reaches much

¹ Primary isotopes are synthesized in stars by nuclear reactions using only H and He as seeds. They thus can be made in stars consisting only of these two elements. In contrast, the synthesis of secondary isotopes requires the prior presence of “metals” (elements heavier than He). As a consequence, primary isotopes are started to be made in the first generation of stars whereas secondary isotopes are made in later generation stars.

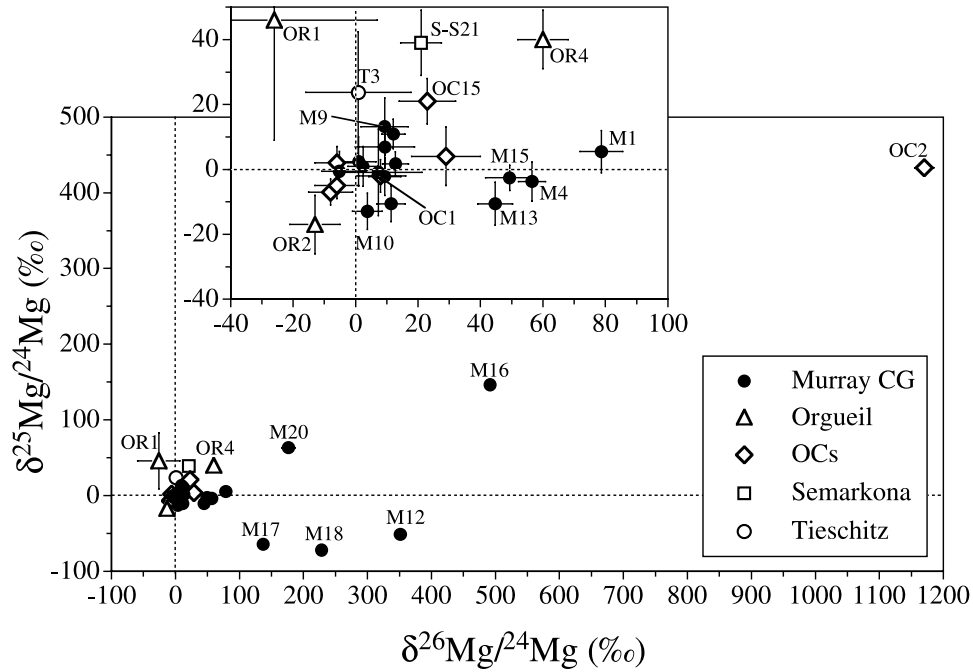


Fig. 2. Magnesium isotopic ratios of presolar spinel grains of this study and of Tieschitz grain T3 (Nittler et al., 1994) and Semarkona grain S-S21 (Choi et al., 1998). The Mg isotopic ratios are plotted as δ -values, deviations from the solar system (terrestrial) ratios ($^{25}\text{Mg}/^{24}\text{Mg} = 0.12663$ and $^{26}\text{Mg}/^{24}\text{Mg} = 0.13932$) in permil (‰). Errors in this figure and in Figures 4, 6 and 7 are 1σ .

deeper zones (Karakas, 2003). Although this ^{26}Al has mostly decayed when the star reaches the TP AGB phase, the decay of ^{26}Al and the depletion in ^{25}Mg during ^{26}Al production alter the Mg isotopic compositions of the stellar envelope. Predicted effects are substantial in more massive stars (^{25}Mg depletion and ^{26}Mg excess of 40 ‰ in a $5M_{\odot}$ star of solar metallicity), whereas the changes in Mg isotopic ratios are only a few permil in $\leq 3.5M_{\odot}$ stars (Karakas, 2003).

The situation is quite different during the AGB phase when the Mg isotopes experience proton-capture reactions in the H-burning shell and have their abundances affected by α -capture on ^{22}Ne , as well as by neutron-capture reactions, in the He-burning shell. Proton-capture reactions affect the Mg isotopes during activation of the Mg-Al chain (Arnould et al., 1999). The first reaction to occur at a temperature of $(30\text{--}35)\times 10^6$ K is the production of the radioisotope ^{26}Al via $^{25}\text{Mg}(p,\gamma)^{26}\text{Al}$. Only 80% of this reaction produces the long-lived ground state, whereas the remaining 20% produces the isomeric state that shortly ($\tau_{1/2} = 6.35$ s) decays to ^{26}Mg . Since the time between thermal cycles in AGB stars is generally shorter than the half life of ^{26}Al , this isotope is

mixed into the envelope by the TDU where it is incorporated live into presolar grains. We thus have to consider the presence of live ^{26}Al when interpreting the Mg isotopic ratios of presolar grains. Evidence for its presence in presolar SiC (Zinner et al., 1991), graphite (Hoppe et al., 1995; Travaglio et al., 1999) and Al_2O_3 (Huss et al., 1992; Hutchison et al., 1994; Nittler et al., 1994) has previously been obtained. Several groups (Forestini et al., 1991; Forestini and Charbonnel, 1997; Mowlavi and Meynet, 2000; Karakas and Lattanzio, 2003) have modeled the production of ^{26}Al and the processes affecting the Mg isotopes in AGB stars and have come to the conclusion that in low-mass AGB stars the production of ^{26}Al (and ^{26}Mg via the isomeric state) and the accompanying destruction of ^{25}Mg dominate among the proton-reaction effects. The reason is that proton capture on ^{24}Mg and ^{26}Mg requires temperatures higher than 60×10^6 K and not much material is dredged up from the regions where such temperatures are reached. As a consequence, ^{27}Al production is low and only in intermediate-mass AGB stars experiencing HBB is the ^{27}Al noticeably increased in the envelope (Forestini et al., 1991; Forestini and Charbon-

Table 2. Chromium isotopic ratios of presolar spinel grains.

Grain	$\delta^{50}\text{Cr}/^{52}\text{Cr}$ (‰) $\pm 1\sigma$	$\delta^{53}\text{Cr}/^{52}\text{Cr}$ (‰) $\pm 1\sigma$	$\delta^{54}\text{Cr}/^{52}\text{Cr}$ (‰) $\pm 1\sigma$
Solar	0.05186	0.11347	0.02821
OC2	26 ± 71	-56 ± 45	102 ± 117
OR1	24 ± 36	-11 ± 24	-115 ± 51
OR2	1 ± 20	3 ± 11	-4 ± 24
OR4	23 ± 53	1 ± 36	-112 ± 86

nel, 1997; Mowlavi and Meynet, 2000; Karakas and Lattanzio, 2003).

In AGB stars, the two heavy Mg isotopes are also produced in the He-burning shell by $^{22}\text{Ne}(\alpha, n)^{25}\text{Mg}$ and $^{22}\text{Ne}(\alpha, \gamma)^{26}\text{Mg}$, where ^{22}Ne is made by $^{14}\text{N}(\alpha, \gamma)^{18}\text{F}(\beta)^{18}\text{O}(\alpha, \gamma)^{22}\text{Ne}$ from the abundant ^{14}N in the ashes of H burning in the CNO cycle. The $^{22}\text{Ne}(\alpha, n)^{25}\text{Mg}$ reaction is actually the neutron source during the thermal pulse. The Mg isotopes are also modified by neutron capture reactions. In addition, ^{26}Al nuclei, produced during previous H-shell burning, are severely affected by the resonant reactions $^{26}\text{Al}(n, p)^{26}\text{Mg}$ and $^{26}\text{Al}(n, \alpha)^{23}\text{Na}$ (Koehler et al., 1997). AGB models that take into account nucleosynthesis in both the H- and He-burning shells predict $^{26}\text{Al}/^{27}\text{Al}$ ratios ranging up to $\sim 2 \times 10^{-3}$ in the envelope of low-mass ($M \leq 3M_{\odot}$) AGB stars (Forestini et al., 1991; Forestini and Charbonnel, 1997; Mowlavi and Meynet, 2000; Karakas and Lattanzio, 2003). Much higher ratios are predicted for more massive stars and stars of lower-than-solar metallicity that experience HBB: up to 0.015 for $6M_{\odot}$ models of solar metallicity, and up to 0.6 for a $6M_{\odot}$ model with $Z = 0.004$ (Mowlavi and Meynet, 2000; Karakas and Lattanzio, 2003). HBB has also a strong effect on the Mg isotopes, resulting in the destruction of ^{24}Mg and large excesses in ^{25}Mg and ^{26}Mg (Karakas and Lattanzio, 2003).

Nollett et al. (2003) have investigated the effect of CBP on the O isotopic ratios and on the production of ^{26}Al in low-mass AGB stars. In their parameterized model, they find that the production of ^{26}Al and the resulting $^{26}\text{Al}/^{27}\text{Al}$ ratio in the star's envelope are mostly determined by the maximum temperature experienced by material circulated to regions close to the H-burning shell and ratios much higher than those reached by the standard AGB models from TDU can be achieved by CBP. On the other hand, the destruction of ^{18}O and the resulting $^{18}\text{O}/^{16}\text{O}$ ratio in the envelope depends mostly on the circulation rate of material through the envelope's hot lower zones. A low $^{18}\text{O}/^{16}\text{O}$ ratio does not necessarily imply a high $^{26}\text{Al}/^{27}\text{Al}$ ratio; the two isotopic systems are in first order decoupled.

4.2. Magnesium and Al Isotopic Ratios and AGB Models

To compare the Mg isotopic ratios of the presolar spinel grains of the present study with theoretical predictions, we have made new calculations of the abundance of the Mg isotopes and of $^{26}\text{Al}/^{27}\text{Al}$ ratios in the envelope of AGB stars. We considered the evolution of the Mg and Al isotopic ratios in the envelope of AGB stars for stellar models with different mass, metallicity, and mass loss during the AGB phase. Here we describe only the most important features of these models. For a general discussion of AGB nucleosynthesis the reader is directed to the review by Busso et al. (1999).

Our calculations made use of a postprocessing code that computes α and neutron captures in the He-burning shell and He intershell (Gallino et al., 1998) and proton captures leading to ^{26}Al production in the H-burning shell. Neutrons are generated by the $^{13}\text{C}(\alpha, n)^{16}\text{O}$ and $^{22}\text{Ne}(\alpha, n)^{25}\text{Mg}$ reactions where the first occurs under radiative conditions during the interpulse period, the second during the recurrent convective thermal pulses taking place in the He- and C-rich intershell. The elemental and isotopic composition of the envelope evolves during the TP-AGB phase because material from the He intershell

and H shell is periodically brought up by TDU. The models do not consider any CBP. Stellar structure parameters such as the envelope mass, the dredged-up mass, the temperature and density at the base of the convective pulse, as well as their trends in time and in mass during the convective TP, are needed as inputs for the postprocessing code. They were obtained for a large number of models from the analytic formulae for AGB stars of masses $\leq 3M_{\odot}$ provided by Straniero et al. (2003). These formulae were generated by interpolating the results of a set of stellar models that were previously evolved using the Frascati RApson Newton Evolutionary Code (FRANEC, Straniero et al., 1997). The $5M_{\odot}$ model was directly obtained from the FRANEC code. Our models cover a range of masses (1.5, 2, 3 and $5M_{\odot}$), metallicities (1/6, 1/3, 1/2 and $1Z_{\odot}$) and Reimers' mass-loss parameters η (ranging from 0.1 to 10 for different stellar masses). Mass loss during the AGB phase was assumed to follow the prescription of Reimers (1975):

$$dM/dt(M_{\odot}/\text{yr}) = 1.34 \times 10^{-5} \eta L^{3/2} / (MT_{\text{eff}}^2) \quad (1)$$

where M is the total mass of the star in solar units, L its luminosity in units of solar luminosity, T_{eff} is the effective temperature (in K) and η is a free parameter. The value of η is assumed to increase with stellar mass because during the AGB phase the strength of stellar winds is observed to increase with the mass of the star (Arndt et al., 1997; Straniero et al., 2005).

For the models with solar metallicity, we assumed solar elemental and isotopic compositions (Anders and Grevesse, 1989) except for the CNO elements for which we adopted the recently suggested abundances (Allende Prieto et al., 2001, 2002). For metallicities lower than solar, the initial compositions of the stars were set by scaling the solar abundance distribution to the Fe abundance of the star for all nuclei except α nuclei, such as ^{16}O , ^{20}Ne , ^{24}Mg , ^{28}Si , whose initial abundances were enhanced, relative to Fe, following the trends observed in F and G stars belonging to the Galactic thin disk (McWilliam, 1997; Reddy et al., 2003). With this assumption the initial $^{25}\text{Mg}/^{24}\text{Mg}$ and $^{26}\text{Mg}/^{24}\text{Mg}$ ratios decrease with decreasing metallicity of the star, reaching values 17%, 28 and 40% lower than the solar ratios at $\text{Fe}/\text{H} = 1/2$, $1/3$ and $1/6$ solar, respectively. The isotopic ratios of most elements affected by the s -process predicted for the envelope of AGB stars crucially depend on the amount of neutrons produced by the ^{13}C source (Lugaro et al., 2003). In contrast, the Mg isotopes are only minimally affected by neutrons from the ^{13}C source. Rather, the Mg isotopic ratios in AGB stars are almost completely determined by capture of neutrons from the ^{22}Ne source and by α -capture reactions on ^{22}Ne . As far as n-capture reactions are concerned, the Mg isotopes behave very similarly to the Si isotopes (Lugaro et al., 1999). As a consequence, models with different amounts of ^{13}C (“ ^{13}C pockets”) yield almost identical results for the Mg isotopic ratios and we plotted only the results obtained from the “standard” ^{13}C pocket (Lugaro et al., 2003).

Figures 3a–d show the evolution of the Mg isotopic ratios in the envelope of stars of 1.5, 2, 3, and $5M_{\odot}$ for solar and half solar metallicity during TDU after individual thermal pulses. Because the envelope becomes increasingly C-rich as more and more ^{12}C produced by He burning is dredged up, the star turns into a carbon star during the TP-AGB phase. Envelope ratios

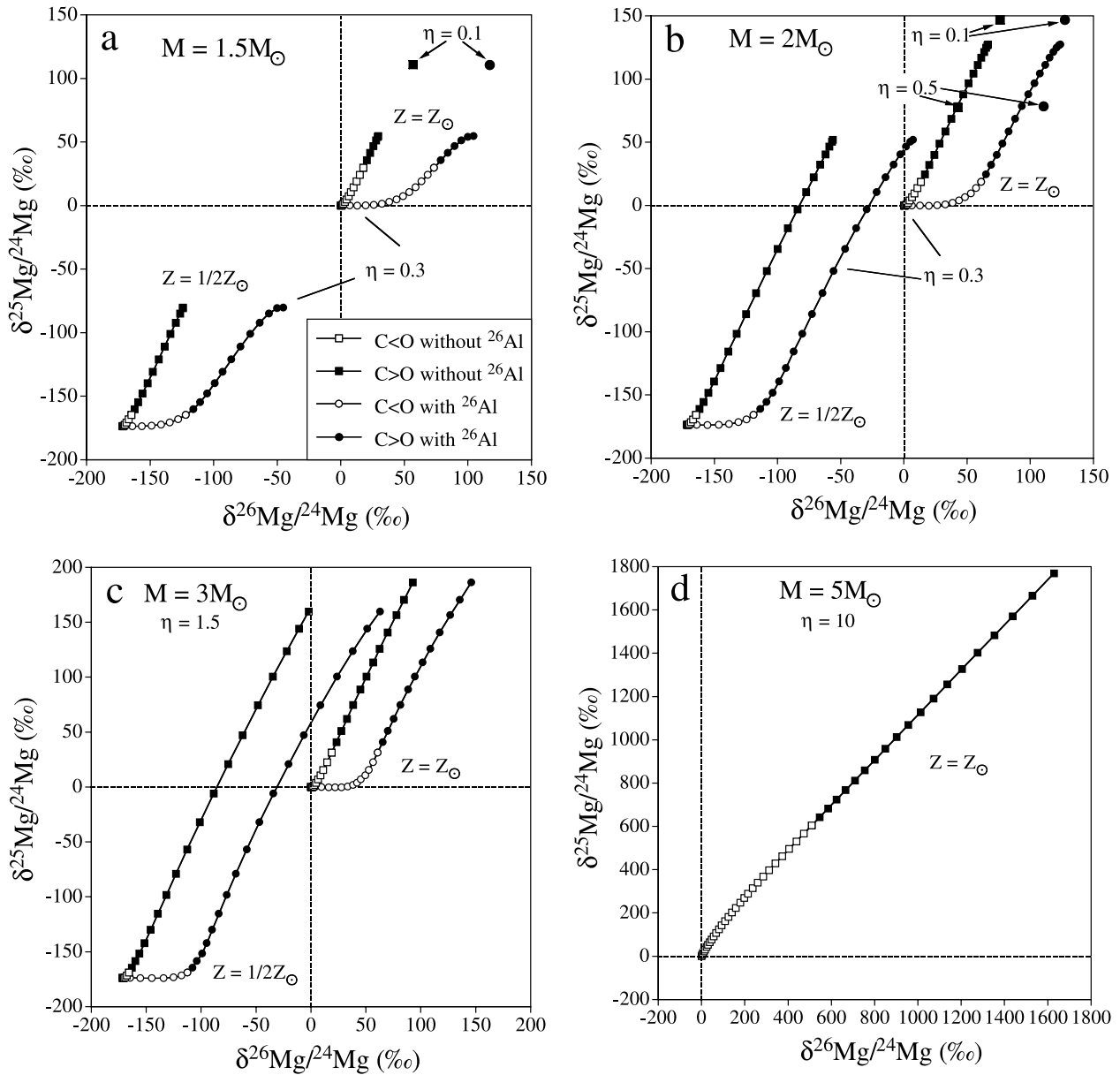


Fig. 3. Predictions for Mg isotopic shifts from models of nucleosynthesis in TP-AGB stars. The models are for different masses (Figs. a–d), metallicities (shown are the cases of solar and half solar metallicity), and Reimers' parameter η for mass loss from the envelope (Figs. a,b). Plotted as squares are the envelope compositions after successive thermal pulses and third dredge-up episodes. The open symbols indicate O-rich (O>C), the filled symbols C-rich (C>O) conditions in the envelope. Oxygen-rich stars produce mostly oxide and silicate grains, C-rich stars mostly carbonaceous grains such as SiC and graphite. Plotted as circles are Mg isotopic ratios resulting from the incorporation and subsequent decay of ^{26}Al in spinel grains with $\text{Al}/\text{Mg} = 2$. For the $1.5M_{\odot}$ (a) and $2M_{\odot}$ (b) cases the evolutionary tracks are shown for $\eta = 0.3$ for both solar and half solar metallicity. The endpoints for other choices of η are shown only for solar metallicity.

before (C<O) and after (C>O) this event are plotted as open and filled symbols. This demarcation is based on the notion that stars with O>C produce oxide grains and those with C>O carbonaceous grains such as graphite and SiC (Larimer and Bartholomay, 1979). However, equilibrium thermochemical calculations suggest that spinel can condense from both O-rich and C-rich atmospheres (Lodders and Fegley, 1995). For the interpretation of the Mg isotopic ratios of spinel grains it is of crucial importance whether or not the grains condensed in the

atmosphere of carbon stars. Corundum and spinel can appear in the condensation sequence of a gas with C>O but only if AlN is not removed by condensation into SiC (Lodders, pers. comm.). If AlN is not removed then it condenses as a separate phase. It is stable only over a small temperature range and at decreasing temperature can be converted into corundum and later into spinel. While detailed calculations that model the kinetic process of condensation in expanding and cooling AGB atmospheres with realistic temperature and pressure profiles are

still outstanding, we believe that carbon stars produced at best only a small fraction of the presolar corundum and spinel grains found in meteorites. First, trace element measurements of presolar SiC grains have shown substantial Al concentrations, indicating that most of the Al indeed condensed into SiC (Amari et al., 1995). Second, the study of pristine presolar SiC grains (Bernatowicz et al., 2003) has shown that condensation of other minerals onto SiC or back-reaction with the gas phase became kinetically inhibited as the gas densities in expanding AGB envelopes became too low. This strongly suggests that conversion into corundum and spinel was also kinetically inhibited. Third, we are not aware of any spectroscopic evidence for Al-rich oxides in the infrared spectra of C stars as there is for O-rich AGB stars (Speck et al., 2000; Sloan et al., 2003). Finally, the systematic difference in the $^{26}\text{Al}/^{27}\text{Al}$ ratios in oxide grains discussed in section 4.6 is additional evidence for an origin of corundum and spinel grains in O-rich stars.

The effect of changing the mass loss rate parameter (i.e., the Reimers' parameter η) is that the excesses in ^{25}Mg and ^{26}Mg become smaller with increasing η (see Figs. 3a and b). The reason is that for a given mass and metallicity a smaller value of η not only increases the number of thermal pulses with dredge-up but also the amount of material that is dredged up per pulse. This property is due to the feedback of the envelope mass on the strength of the TDU: the smaller η is, the larger is the mass of the envelope at a given TP and consequently the higher the dredged-up mass per pulse. This effect dominates the fact that with a lower mass loss rate the envelope mass remains larger and the dredged-up material is diluted more than for a larger mass loss rate. The slope of the evolution of the Mg isotopes in a Mg 3-isotope diagram does not depend on Reimers' parameter nor does it appear to depend significantly on stellar mass and metallicity for the $\leq 3M_{\odot}$ models. For these masses, in the diagrams without any ^{26}Al contribution in Figures 3a-c the evolutionary tracks of the Mg isotopes have slopes between 1.9 and 2.0. This holds also for different η values, for which only the endpoints of the evolutionary tracks are shown in the figures. For the $5M_{\odot}$ model the slope is 1.15 (Fig. 3d). In the figures, we also plot the Mg isotopic ratios expected in spinel grains after decay of ^{26}Al that was incorporated during condensation of these grains. Excesses in ^{26}Mg due to ^{26}Al decay become larger with increasing mass-loss rate. Because the Al/Mg ratio in spinel is ~ 25 times that in the stellar envelope (the Al/Mg ratio in spinel is 2 but the solar ratio is only 0.079; Anders and Grevesse, 1989), the ^{26}Mg excesses expected from ^{26}Al decay are larger by this factor than the excesses resulting from decay in the stellar atmosphere. Predicted excesses for spinel are $\sim 80\%$ for the $1.5 M_{\odot}$ model when C/O has reached unity and become smaller for higher masses (Fig. 3).

4.3. Grain Data and AGB Models

A comparison of the theoretical models discussed in the previous sections and the selected data on presolar spinel grains is shown in Figures 4a and b. There are several explanations for grain data points close to the normal isotopic ratios: 1) These grains could be from RGB stars, in which case their Mg isotopic compositions were not modified by any stellar nucleosynthesis and represent those of their parent stars whose isoto-

pic compositions were close to solar. 2) The grains are from stars that didn't experience any TDU during the AGB phase. 3) The parent stars experienced *some* TDU and the observed compositions agree with predicted compositions within the error bars. The Mg isotopic compositions of grains with some relative ^{26}Mg excesses, such as OR4, M1, M4, M13 and M15 (Table 1 and Fig. 2), can be successfully explained by the AGB models; those of M13 would require a parent star of slightly subsolar metallicity. However, the ^{26}Mg excesses in the grains M12, M16, M17, M18, M20, and especially OC2 are much larger than predictions by the AGB models. They are most likely from the decay of ^{26}Al incorporated into the grains, but imply much higher $^{26}\text{Al}/^{27}\text{Al}$ ratios than are predicted by models of proton capture in the H-burning shell of AGB stars.

In Table 1, we give $^{26}\text{Al}/^{27}\text{Al}$ ratios inferred from the Mg isotopic ratios by assuming that any shift to the right of the model predictions for the envelope Mg ratios (without ^{26}Al contributions) is due to in situ ^{26}Al decay. To obtain the radiogenic excess for a given grain, we project the Mg isotopic ratio of this grain back to a model composition. This is done along a trajectory with slope $-1/20$ because 80% of ^{25}Mg capturing a proton is turned into ^{26}Al and because the Al/Mg ratio in spinel is 25 times as high as in the envelope (the latter is assumed to be solar). However, this prescription is not unambiguous, as can be seen in Figure 4a. For example, according to its Mg isotopic composition the spinel grain M16 could come from a $3M_{\odot}$ star with solar metallicity Z_{\odot} or from a star with the same mass but $1/2Z_{\odot}$ (however, see discussion below about constraints coming from O isotopic ratios). Similarly, grain M18 could have originated from stars with a range of metallicities. Correspondingly, for both grains the inferred radiogenic ^{26}Mg excesses and thus $^{26}\text{Al}/^{27}\text{Al}$ ratios are not uniquely defined. For Table 1, we use the minimum values indicated by asterisks in Figure 4a. For grains with ^{25}Mg excesses, radiogenic ^{26}Mg excesses and inferred $^{26}\text{Al}/^{27}\text{Al}$ ratios were obtained by projecting the Mg ratios to compositions of models with solar metallicity. We used a line with slope 1.95 passing through the origin based on the stellar models summarized in Figures 3a-c. For grains with ^{25}Mg deficits, we projected the Mg ratios to the line with slope one through the normal ratios. This line represents the Galactic evolution track of the Mg isotopes and using it assumes that no significant modification of the Mg isotopes due to He burning had taken place yet.

A comparison of the AGB models with the Mg grain data also does not provide a unique identification of the masses of the parent stars. Because the maximum ^{25}Mg excess predicted for an O-rich (O>C) envelope in any of the $\leq 3M_{\odot}$ models with solar metallicity is only 40‰ (Figs. 3a-c), the grains M20 and M16 can only come from $\leq 3M_{\odot}$ and solar metallicity stars if they condensed from an atmosphere with C>O. This assumes no ^{25}Mg excess in the parent stars of these grains. Although condensation of spinel from a C-rich gas is thermodynamically possible (Lodders and Fegley, 1995), as discussed above, the question is how likely this is going to be, especially for a gas where the C/O ratio can be as high as 2.

We can use the O isotopic data to obtain information about the mass and metallicity of the parent stars of the grains. Boothroyd and co-workers (Boothroyd et al., 1994; Boothroyd and Sackmann, 1999) presented a grid of predicted O isotopic

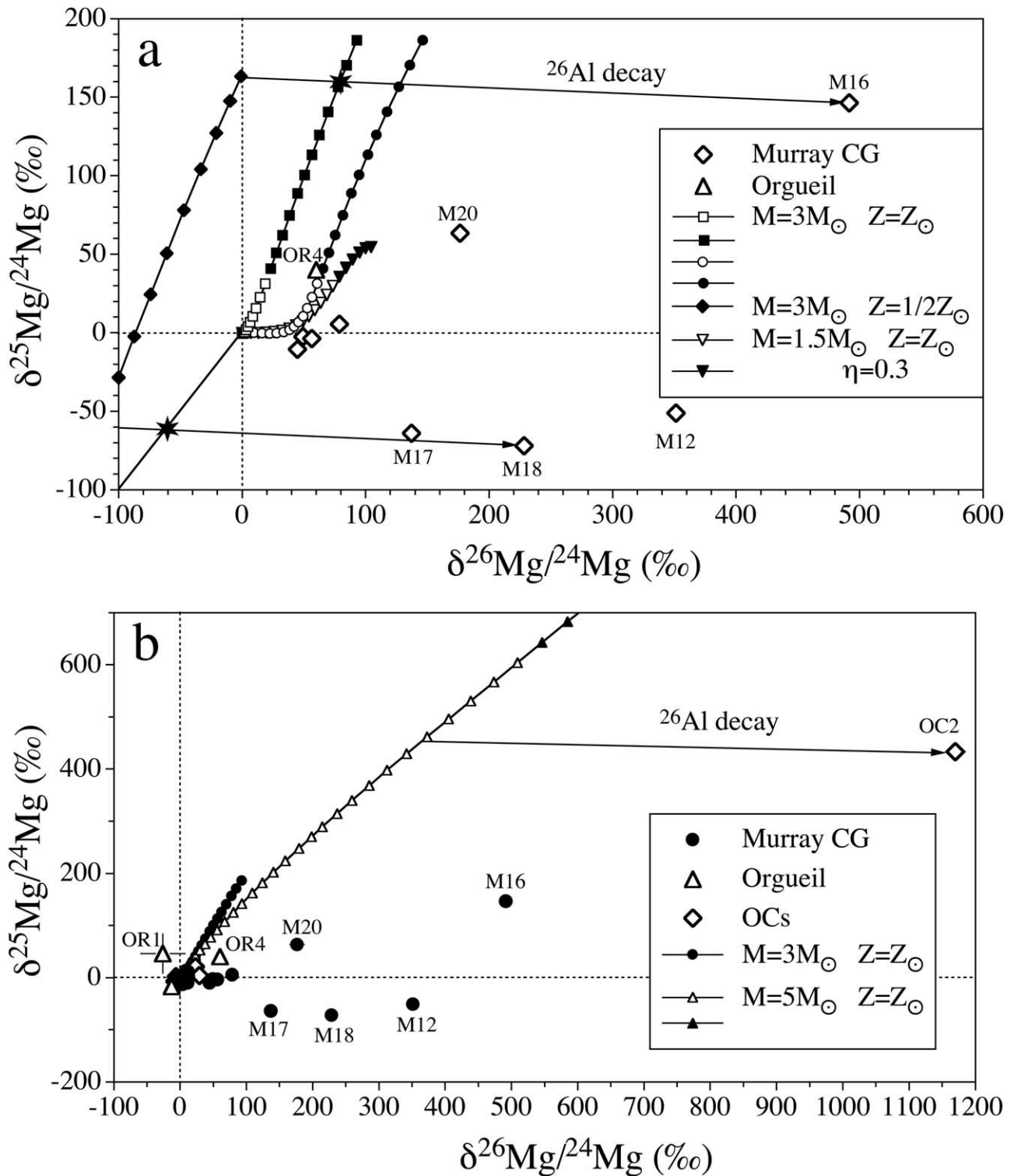


Fig. 4. Magnesium isotopic ratios measured in presolar spinel grains are compared with predictions from AGB models. Figure 4a shows model predictions for a 3M_⊙ star with Z_⊙ with (circles) and without (squares) ²⁶Al decay, 3M_⊙ star with 1/2Z_⊙ without ²⁶Al decay, and a 1.5M_⊙ star with Z_⊙ and ²⁶Al decay, Figure 4b shows also model predictions for a 5M_⊙ star with Z_⊙ and O>C. As in Figure 3, open symbols for the predictions represent O-rich, filled symbols C-rich conditions. The large ²⁶Mg excesses of some of the grains are interpreted to originate from ²⁶Al decay; shifts due to ²⁶Al production resulting in ²⁵Mg depletion and ²⁶Al decay are shown by lines with arrows. Assumed initial compositions used to calculate ²⁶Al/²⁷Al ratios are indicated by asterisks.

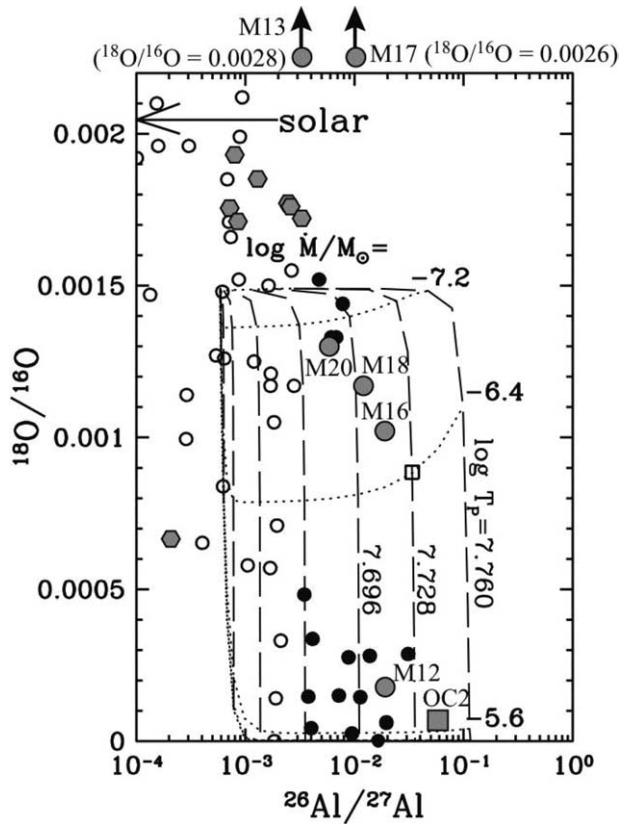


Fig. 5. Copy of Figure 6 from Nollert et al. (2003) with the superimposed isotopic compositions of the spinel grains from this study. Grains for which cool bottom processing has to be invoked to explain their inferred $^{26}\text{Al}/^{27}\text{Al}$ ratios are represented by large circles with grey shadings, grains for which no CBP is required by hexagons. The unique grain OC2 (large square) is probably from a star that experienced HBB. The original Nollert et al. plot shows theoretical predictions for the $^{18}\text{O}/^{16}\text{O}$ and $^{26}\text{Al}/^{27}\text{Al}$ ratios in the envelope of TP-AGB stars undergoing CBP. The dotted and dashed lines indicate different values for the circulation rate of material through hot layers close to the H-burning shell and the maximum temperature reached, respectively. The open and filled small circles are previous data from corundum grains (Nittler et al., 1997; Choi et al., 1998).

ratios for red giants of different masses and metallicities, taking into account expected changes from Galactic chemical evolution (GCE) and the first and second dredge-ups. By interpolating measured isotopic compositions in this grid, one can infer the mass and metallicity of the parent star of each grain (Nittler et al., 1997; Alexander and Nittler, 1999; Nittler, 2005). The inferred metallicities are discussed below in Section 4.5. The predicted $^{17}\text{O}/^{16}\text{O}$ ratio following first dredge-up depends strongly on the stellar mass, and thus it is this ratio that most strongly influences the inferred masses. For stars more massive than $\sim 1.5M_{\odot}$, the predicted $^{17}\text{O}/^{16}\text{O}$ ratio is relatively insensitive to the initial ratio of the star. However, for less massive stars, the final ratio does depend on the initial composition, which is assumed from Galactic chemical evolution models (see Section 4.5). Thus, the inferred masses (especially those below $1.5M_{\odot}$) potentially have large systematic uncertainties and the reported values should be taken with a grain of salt. However, we can say with some certainty that all of the parent stars of the group 1 and 3 spinel grains were less massive than

$2M_{\odot}$, or they would have much higher $^{17}\text{O}/^{16}\text{O}$ ratios than observed. A lower limit of $1.1M_{\odot}$ may also be assumed, based simply on the fact that lower mass stars would not have had time to evolve to the red giant stage (Lampens et al., 1997; Martin et al., 1998) during the ~ 8 billion years that the Milky Way disk existed before the formation of the solar system (Bennett et al., 2003; Krauss and Chaboyer, 2003).

Inferred masses of group 1 and 3 grains are given in Table 1. For example, the O isotopic ratios (mostly the $^{17}\text{O}/^{16}\text{O}$ ratio) of grain M16 indicate a parent-star mass of only $1.55M_{\odot}$. As can be seen in Figure 3a, according to the AGB models a $1.5M_{\odot}$ star does not produce the ^{25}Mg excess observed in this grain even for a Reimers' parameter of 0.1. Most of the ^{25}Mg excess in this grain thus most likely reflects the initial composition of the parent star and has a GCE origin. If we assume that the parent star had an isotopic composition that lies on a slope-one line and had positive δMg values, i.e., that the GCE extends beyond the solar composition, it can be easily seen from Figure

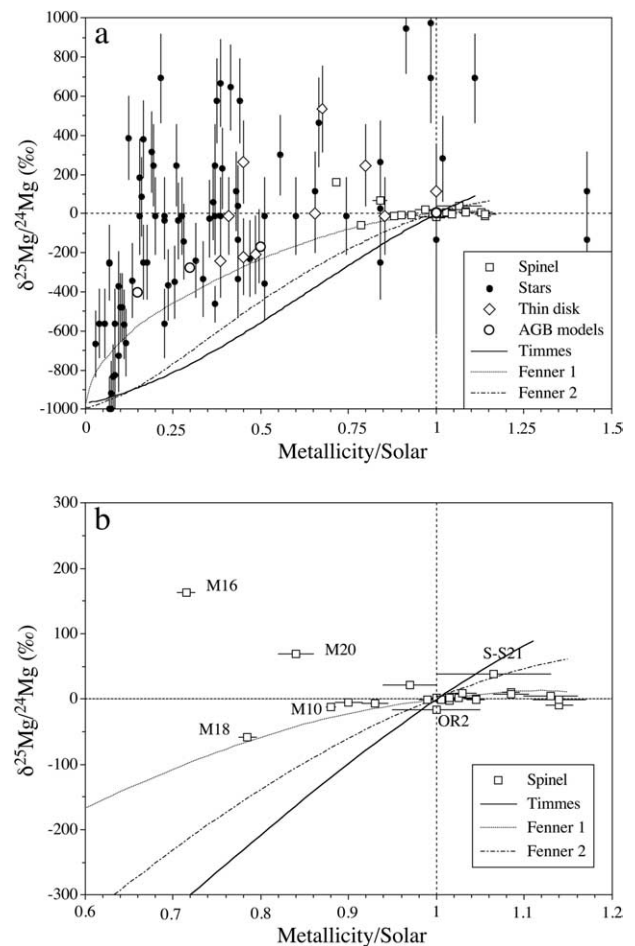


Fig. 6. The $^{25}\text{Mg}/^{24}\text{Mg}$ ratios of presolar spinel grains are plotted vs. the initial metallicities of their parent stars inferred from their O isotopic ratios. Also shown are astronomical observations of stars (McWilliam and Lambert, 1988; Gay and Lambert, 2000; Yong et al., 2003), the assumed ratios for our AGB models and theoretical predictions from GCE models by Timmes et al. (1995) and Fenner et al. (2003), the latter with (Fenner 1) and without (Fenner 2) contributions from AGB stars. Of the Yong et al. (2003) data we plot the thin-disk stars separately.

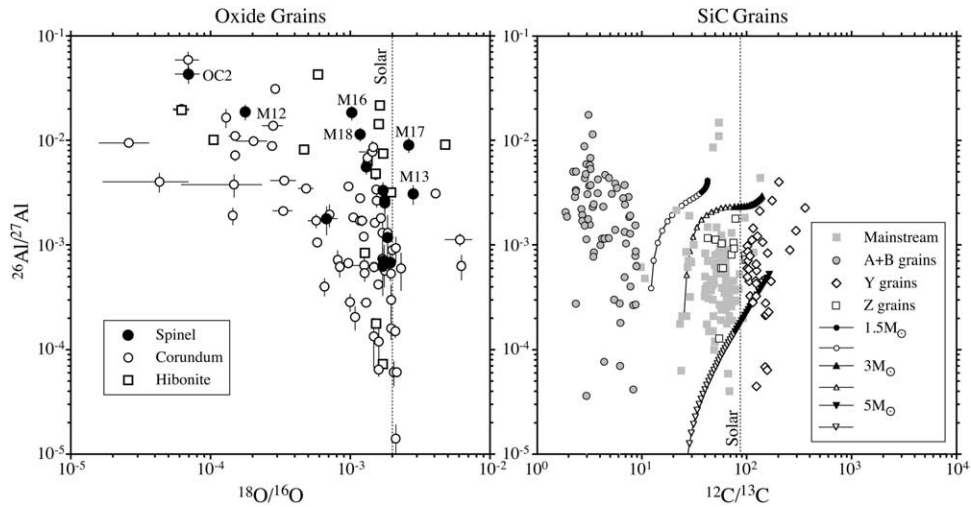


Fig. 7. Comparison of inferred $^{26}\text{Al}/^{27}\text{Al}$ ratios in presolar oxide grains and SiC grain types believed to be from AGB stars as well as grains of type A+B. In the SiC plot we also show the predictions from our AGB models for the envelope compositions of TP-AGB stars with $C < O$ (open symbols) and $C > O$ (solid symbols) for sequential thermal pulses and third dredge-up. Data for the oxide grains are from Nittler et al. (1997), Choi et al. (1998, 1999) and the present study. Data for the SiC grains are from Hoppe et al. (1994, 2000), Nittler et al. (1995, 2005), Amari et al. (2001a, 2001b, 2001c) and Zinner et al. (2005).

4a that in this case the inferred $^{26}\text{Al}/^{27}\text{Al}$ ratio would be lower (1.7×10^{-2} instead of the 2.0×10^{-2} given in Table 1).

Grain OC2, which belongs to group 2, has to come from a star more massive than $3M_{\odot}$ in any case. Our $5M_{\odot}$ model achieves high enough ^{25}Mg excesses to explain the excess observed in OC2 even for $O > C$. A $5M_{\odot}$ mass star is likely to experience HBB (Boothroyd et al., 1995; Lattanzio et al., 2000), especially for subsolar metallicity, although in our $5M_{\odot}$ model of solar metallicity based on the FRANEC code we do not achieve it and in the $5M_{\odot}$ model HBB occurs only at $1/6Z_{\odot}$. In such a star, at high enough temperatures, ^{25}Mg excesses are also generated by proton capture on ^{24}Mg . The $4M_{\odot}$ model with solar metallicity of Karakas and Lattanzio (2003) indicates already some destruction of ^{24}Mg . In addition, the inferred $^{26}\text{Al}/^{27}\text{Al}$ ratio of 0.04 in OC2 is consistent with HBB calculations (Mowlavi and Meynet, 2000). Thus, an intermediate-mass AGB star that experienced HBB is an attractive candidate as parent star of grain OC2. The question is whether a consistent set of conditions can be found that also explain the O isotopic ratios in this grain. However, this is beyond the scope of this paper and we will pursue this question independently.

4.4. Cool Bottom Processing

The ^{26}Mg excesses observed in several of the spinel grains of this study are larger than can be explained by our standard AGB models. They have to be attributed to extra production of ^{26}Al . For grain OC2, HBB has been considered above. For the other grains with large inferred $^{26}\text{Al}/^{27}\text{Al}$ ratios, the most likely cause for this extra production is CBP. Nollett et al. (2003) have calculated the effect of CBP on the O isotopic ratios and on the production of ^{26}Al from a parametric model for TP-AGB stars. In Figure 5 we have taken Figure 6 of the Nollett et al. (2003) paper and superimposed the $^{18}\text{O}/^{16}\text{O}$ and inferred $^{26}\text{Al}/^{27}\text{Al}$ ratios of the presolar spinel grains determined in this study. The plot shows predictions

for these two isotopic ratios for different values of the two parameters of the CPB model, the rate of mass circulation dM/dt and the maximum temperature T_p . The $^{18}\text{O}/^{16}\text{O}$ ratio depends mostly on the mass circulation rate whereas the $^{26}\text{Al}/^{27}\text{Al}$ ratio depends predominantly on T_p . The original plot also contained the isotopic ratios of presolar corundum grains plotted as open (grains with $^{26}\text{Al}/^{27}\text{Al} < 2 \times 10^{-3}$) and filled (grains with $^{26}\text{Al}/^{27}\text{Al} > 2 \times 10^{-3}$) circles.

With the exception of OC2, the inferred $^{26}\text{Al}/^{27}\text{Al}$ ratios of the spinel grains do not exceed those of the corundum grains, although grains M16 and M18 have higher $^{18}\text{O}/^{16}\text{O}$ ratios than corundum grains with comparable $^{26}\text{Al}/^{27}\text{Al}$ ratios. Grain M17 is exceptional in that it has an $^{18}\text{O}/^{16}\text{O}$ ratio greater than solar, i.e., it belongs to group 4, but it has a ^{26}Mg excess that is larger than our standard AGB models (without CBP) can explain. The parent star could not have experienced HBB because that would have resulted in large ^{18}O depletions. Group 4 grains with moderate ^{17}O and ^{18}O excesses have been interpreted to possibly have an origin in AGB stars with higher-than-solar metallicity (Nittler et al., 1997), but grain M17 has a ^{25}Mg deficit, indicating a parent star of low metallicity. Recently, Nittler et al. (2005) found a hibonite grain with an even larger ^{18}O excess and an $^{26}\text{Al}/^{27}\text{Al}$ ratio comparable to that of M17 (Fig. 7). This grain also has a ^{25}Mg deficit. At present, we do not have a satisfying explanation for the O and Mg isotopic compositions of these two grains (or, for that matter, for group 4 grains in general).

4.5. Galactic Chemical Evolution (GCE)

In principle, both the O and Mg isotopic ratios of presolar oxide grains are expected to reflect the initial ratios of the parent stars in addition to changes that occurred due to nucleosynthetic processes during the subsequent evolution of these stars. As discussed above in Section 4.3, we have inferred the

metallicities of the parent stars of the group 1 and 3 spinel grains from their O isotopic ratios and the models of Boothroyd and Sackmann (1999). Note that the metallicity is mostly inferred from the grains' $^{18}\text{O}/^{16}\text{O}$ ratios, since the $^{17}\text{O}/^{16}\text{O}$ ratios are much more severely affected by dredge-up. However, the GCE of ^{18}O is not quantitatively well understood (Prantzos et al., 1996). Observations of molecular clouds indicate that this isotope behaves as a secondary isotope, so that grains with lower $^{18}\text{O}/^{16}\text{O}$ ratios originated in stars of lower metallicity than did grains with higher $^{18}\text{O}/^{16}\text{O}$ ratios, but the precise relationship between $^{18}\text{O}/^{16}\text{O}$ and metallicity is unknown. Boothroyd and Sackmann (1999) assumed that the $^{18}\text{O}/^{16}\text{O}$ ratio of the Galaxy scales linearly with the Fe/H ratio (Timmes et al., 1995), and in the absence of a better model, we also make this assumption in inferring parent star metallicities.

By taking into account the theoretically expected changes in the O isotopic ratios due to the first and second dredge-up (Boothroyd et al., 1994; Boothroyd and Sackmann, 1999), Nittler and coworkers determined the initial O ratios of the parent stars of oxide grains from groups 1 and 3 (Nittler et al., 1997; Alexander and Nittler, 1999; Nittler, 2005). From these ratios and galactic evolution models of the $^{18}\text{O}/^{16}\text{O}$ ratio (Timmes et al., 1995) they inferred the metallicity of these parent stars (see also Nittler, 1997).

Galactic evolution is expected to also affect the Mg isotopic ratios (Timmes et al., 1995; Goswami and Prantzos, 2000; Alibés et al., 2001; Fenner et al., 2003). For our AGB models (Figs. 3a-c) we assumed different initial Mg isotopic ratios for stars of different metallicity.

It is therefore tempting to use the O and Mg isotopic data of presolar spinel grains to obtain information on the GCE of the Mg isotopes. We can use the O isotopic ratios of group 1 and 3 grains to infer the metallicity of their parent stars (Nittler et al., 1997) and then assume that variations in the $^{25}\text{Mg}/^{24}\text{Mg}$ ratios exhibited by the grains are dominated by GCE effects and not by nucleosynthesis in the AGB parent stars. The $^{26}\text{Mg}/^{24}\text{Mg}$ ratios are not useful because they are apparently strongly affected by the decay of ^{26}Al . However, it is far from clear that even the $^{25}\text{Mg}/^{24}\text{Mg}$ ratio is a good monitor of GCE as long as we allow spinel grains to condense from a gas with $\text{C}>\text{O}$. This can be clearly seen in Figure 4a. For example, let us ask what the initial $^{25}\text{Mg}/^{24}\text{Mg}$ ratio of the parent star of grain M18 was. If the $^{25}\text{Mg}/^{24}\text{Mg}$ ratio in this star was modified only by ^{26}Al production from proton capture on ^{25}Mg , then the initial Mg isotopic ratios are represented by the asterisk in the figure, i.e., the initial $\delta^{25}\text{Mg}/^{24}\text{Mg}$ value was -65% . However, according to our AGB models, grain M18 could have had its origin in a star with a much lower initial $^{25}\text{Mg}/^{24}\text{Mg}$ ratio that was increased during the TP-AGB phase along the track shown in Figure 3c for the $M = 3M_{\odot}$, $1/2Z_{\odot}$ model. Above, we already discussed this basic ambiguity in connection with the determination of the ^{26}Mg excesses due to ^{26}Al decay. This situation improves if spinel grains formed only from a gas with $\text{O}>\text{C}$. As can be seen from the theoretical predictions (Figs. 3a-d), except for the $M = 5M_{\odot}$, Z_{\odot} model, the shifts in the Mg isotopic ratios due to AGB nucleosynthesis are rather modest as long as $\text{O}>\text{C}$.

We make the simplifying assumption that the $^{25}\text{Mg}/^{24}\text{Mg}$ ratios in the parent stars of our spinel grains were not modified from the initial ratios, except for the depletion of ^{25}Mg accompanying the production of ^{26}Al . In Figures 6a and b, we plot

these “initial” $^{25}\text{Mg}/^{24}\text{Mg}$ ratios vs. the metallicity inferred from their O isotopic ratios for group 1 and 3 grains. We compare these ratios with stellar data (McWilliam and Lambert, 1988; Gay and Lambert, 2000; Yong et al., 2003) and with the theoretical prediction of GCE models of the Mg isotopes by Timmes et al. (1995) and Fenner et al. (2003). Fenner et al. (2003) performed calculations both with (Fenner 1) and without (Fenner 2) including nucleosynthetic contributions from AGB stars. Also shown are the initial $^{25}\text{Mg}/^{24}\text{Mg}$ ratios that were assumed in our models for AGB stars of different metallicities. Of the Yong et al. (2003) data we plot the thin-disk stars separately. These authors noticed that the Mg isotopic compositions of thin-disk stars agree better with GCE models than those of thick-disk and halo stars, which show a much larger scatter. The Sun and most stars in the solar neighborhood and all population I stars belong to the thin disk, which has a scale height of 200–300 pc. Presolar grains most likely come from stars in the thin disk. Stars in the thick (~ 1 kpc) disk, and especially the halo stars, are old stars with metallicities much lower than that of the Sun. Their abundances in the solar neighborhood are only 2% and a few permil, respectively, and they are believed to have contributed only marginally to the chemical evolution of the Galaxy. For more details see the contributions by Fuhrmann (1998) and Bensby et al. (2003; 2004).

We note that we normalized the predictions of the GCE models plotted in Figure 6 so that the $^{25}\text{Mg}/^{24}\text{Mg}$ ratios are normal (i.e., $\delta^{25}\text{Mg}/^{24}\text{Mg} = 0$) for solar metallicity. The unnormalized models of Fenner et al. (2003) actually predict $\delta^{25}\text{Mg}/^{24}\text{Mg}$ values of 562‰ with AGB contributions, and 381‰ without any AGB contributions, at solar metallicity. The grain data, which strictly speaking are upper limits because of the possibility of enhancements from dredge-up, exclude such high values and provide justification for our normalization.

While the GCE models predict a decrease of $\delta^{25}\text{Mg}/^{24}\text{Mg}$ for lower than solar metallicities, two grains with subsolar metallicity according to their O isotopes as well as a number of stars have ^{25}Mg excesses relative to the solar $^{25}\text{Mg}/^{24}\text{Mg}$ ratio. Of course, these two grains, M16 and M20, could have come from stars with initially smaller $^{25}\text{Mg}/^{24}\text{Mg}$ ratios that were increased by AGB nucleosynthesis. The parent-star mass of $1.55M_{\odot}$ obtained for grain M16 from its O isotopic ratios (Table 1) sets a limit of $\delta^{25}\text{Mg}/^{24}\text{Mg} = \sim 100\%$ for a mass loss parameter $\eta = 0.1$ and $\delta^{25}\text{Mg}/^{24}\text{Mg} = \sim 50\%$ for $\eta = 0.3$ (see Fig. 3a). However, these limits apply to an envelope with $\text{C}>\text{O}$ and, as discussed earlier, for stars with masses $\leq 3M_{\odot}$ the ^{25}Mg excesses found in grains M16 and M20 would require formation from a gas with $\text{C}>\text{O}$. While Lodders and Fegley (1995) predict condensation of spinel from a gas with $\text{C}/\text{O} = 1.05$, the question is whether this is also the case for much higher C/O ratios. According to our AGB models, for a $3M_{\odot}$ star of solar metallicity, the ^{25}Mg excess observed in grain M16 implies a C/O ratio of 1.68. Even if spinel can condense from a gas with such a high ratio, we argued above that the spinel grains most likely originated in O-rich stars. The difference in the average $^{26}\text{Al}/^{27}\text{Al}$ ratios of oxide grains discussed below provides additional evidence.

As can be seen from Figure 3d, $^{25}\text{Mg}/^{24}\text{Mg}$ ratios in the $5M_{\odot}$ model are high enough to account for the ^{25}Mg excesses in M16 and M20 under $\text{O}>\text{C}$ conditions. However, the $^{17}\text{O}/^{16}\text{O}$

ratios in all the group 1 and 3 grains of this study including grains M16 and M20 indicate low-mass parent stars with masses $<2M_{\odot}$. It could be that CBP prevents an AGB star from turning into a carbon star and these grains could be from stars of lower mass, but that would require a high circulation rate (Nollett et al., 2003), resulting in lower $^{18}\text{O}/^{16}\text{O}$ ratios than those observed in these two grains. This scenario, however, is not without problems, because the rare SiC Z grains apparently formed in low-metallicity C-rich AGB stars which experienced strong CBP during the red giant phase (Hoppe et al., 1997; Nittler and Alexander, 2003a). The alternative, that not CBP but HBB is responsible for the ^{26}Al in these grains, is unlikely because this process would also result in extremely low $^{18}\text{O}/^{16}\text{O}$ ratios. A final, and in our view most likely, alternative is that the initial $^{25}\text{Mg}/^{24}\text{Mg}$ ratios of the parent stars of grains M16 and M20 were substantially higher than solar. Mainstream SiC grains have excesses in ^{29}Si and ^{30}Si that cannot be explained by AGB nucleosynthesis and have been attributed to the initial Si isotopic compositions of their parent stars, which were determined by GCE (Lugaro et al., 1999; Alexander and Nittler, 1999). Thus it is to be expected that presolar spinel grains have corresponding ^{25}Mg excesses. The fact that many low-metallicity main-sequence stars, even thin-disk stars (Fig. 6a), have ^{25}Mg enrichments relative to solar is consistent with this possibility.

Grain M18 plots close to the prediction of the Fenner et al. GCE model including contributions from AGB stars (Fenner 1, Fig. 6b). As is the case for the other grains, the parent star of this grain could in principle have had a smaller initial $^{25}\text{Mg}/^{24}\text{Mg}$ ratio. Here we also could go through the same discussion as for grains M16 and M20. Grain M18 also has an inferred $^{26}\text{Al}/^{27}\text{Al}$ ratio that implies CBP and its mass inferred from the O isotopic ratios is only $1.56M_{\odot}$ (Table 1). If we apply the same argument as above about the low likelihood that this grain condensed from a carbon star, the $^{25}\text{Mg}/^{24}\text{Mg}$ ratio in M18 appears to exclude the Timmes et al. (1995) model and Fenner et al. (2003) model without AGB contributions. As can be seen from Figure 6, most of the spinel grains with close-to-solar $^{25}\text{Mg}/^{24}\text{Mg}$ ratios and metallicity greater than solar, as well as the stellar data, also seem to favor the Fenner et al. model with AGB contributions.

From these discussions, we arrive at these tentative conclusions: Although spinel can, in principle, condense from a gas with $\text{C}/\text{O} > 1$, it is most likely that most of the spinel grains originated in O-rich low-mass stars. If this is the case, the variations in the $^{25}\text{Mg}/^{24}\text{Mg}$ ratios are dominated by GCE effects and AGB nucleosynthesis contributes mostly to the production of ^{26}Al but the effect on the Mg isotopes is minor. This situation is similar to that of the Si isotopic ratios in mainstream SiC grains where the initial isotopic compositions of the parent stars dominate (Hoppe and Ott, 1997; Lugaro et al., 1999). Only grain OC2 seems to have an origin in an intermediate-mass AGB star.

At present, a better understanding of several problems is required before we can fully exploit the information contained in the Mg isotopic compositions of presolar spinel grains. One is the question at which C/O ratios spinel can condense and how much of it is produced at different C/O ratios. Ebel (2000) calculated condensation temperatures of various minerals for C/O ratios ranging from 0.8 to 1.15. Although he did not

include spinel, his results show that for $\text{C}/\text{O} > 1.05$ the condensation temperature of corundum and other oxides is constant. It is therefore highly desirable to extend condensation calculations to higher C/O ratios and to include spinel to see whether or not forsterite condensation prevents the appearance of spinel. However, as already discussed, the probability that presolar spinel grains originated from carbon stars is small. We also wish for detailed studies under which conditions CBP can prevent the formation of a carbon star and what the resulting change in O isotopic ratios would be if this is the case. We also need more detailed investigations of HBB. In our $5M_{\odot}$ FRANEC model we do not obtain HBB whereas other stellar evolution models achieve it at this mass (Lattanzio et al., 2000). It is also desirable to have a finer mass grid for AGB nucleosynthesis models. In our models there is a large difference in the isotopic shifts due to AGB nucleosynthesis between the $3M_{\odot}$ and $5M_{\odot}$ models.

4.6. $^{26}\text{Al}/^{27}\text{Al}$ Ratios in Presolar Oxide and SiC

Several presolar spinel grains of this study have inferred $^{26}\text{Al}/^{27}\text{Al}$ ratios that are larger than those that are predicted in our AGB models without CBP. This feature is not restricted to spinel grains but is also observed in other presolar oxide grains. In Figure 7 we compare the inferred $^{26}\text{Al}/^{27}\text{Al}$ ratios in oxide grains with those measured in presolar SiC grains. We also plot the predictions for $^{12}\text{C}/^{13}\text{C}$ and $^{26}\text{Al}/^{27}\text{Al}$ ratios from our AGB models. The inferred $^{26}\text{Al}/^{27}\text{Al}$ ratios in oxide grains reach much higher values than those in SiC grains believed to come from AGB stars: mainstream, Y and Z grains. Only three mainstream grains have higher $^{26}\text{Al}/^{27}\text{Al}$ ratios than the models predict, all the others plot below the predicted ratios. The A+B grains reach higher values. The low $^{12}\text{C}/^{13}\text{C}$ ratios of these grains must be the result of H burning in the CN cycle and temperatures must have been high enough to produce substantial amounts of ^{26}Al . However, we still do not know exactly in which stellar environment these processes occurred (Amari et al., 2001c). The $^{26}\text{Al}/^{27}\text{Al}$ ratios of the oxide grains reach even higher values, up to 0.06 and thus overlap with the $^{26}\text{Al}/^{27}\text{Al}$ ratios exhibited by SiC grains from novae (Amari et al., 2001a) and supernovae (the X grains) (Nittler et al., 1995; Hoppe et al., 2000). Although there is considerable scatter, the $^{26}\text{Al}/^{27}\text{Al}$ ratios in the oxide grains tend to decrease with increasing $^{18}\text{O}/^{16}\text{O}$ ratios. This is not unexpected because proton-capture reactions produce ^{26}Al and destroy ^{18}O , however some circulation of envelope material through the hot zones experiencing H burning as envisioned in the CBP model must have occurred to lower the $^{18}\text{O}/^{16}\text{O}$ ratio of the whole envelope. Shell burning alone and subsequent dredge-up would not accomplish a large-scale overall change in the O isotopic ratio.

The fact that oxide grains reach substantially higher $^{26}\text{Al}/^{27}\text{Al}$ ratios than SiC grains from AGB stars is somewhat surprising. The $^{17}\text{O}/^{16}\text{O}$ ratios of most presolar oxide grains, including the spinel grains of the present study, indicate that they are from low-mass ($\leq 2M_{\odot}$) RGB and AGB stars (Nittler et al., 1997). Likewise, there is abundant evidence that mainstream SiC come from low-mass AGB stars (Gallino et al., 1997; Lugaro et al., 2003). Thus, it might be expected that the same stars that produced oxide grains when they were O-rich could have produced the mainstream, Y and Z grains once they

turned into carbon stars. If this were true, however, and even in the unlikely case that corundum and spinel grains formed from carbon stars, one would expect that $^{26}\text{Al}/^{27}\text{Al}$ ratios in the SiC grains would be at least as high as in the oxide grains and our AGB models without CBP predict a continuous increase of the $^{26}\text{Al}/^{27}\text{Al}$ ratios in the envelope with increasing pulse number. However, this is clearly not the case and the stars that produced the oxide and SiC grains differ from one another in some fundamental way and are not the same stars at different stages in their evolution. One possible difference might be the masses of the parent stars. For example, if there is a cutoff around $2M_{\odot}$ for a star to become C-rich, then the steep initial mass function, the birth rates of stars with different masses (Scalo, 1986), suggests that the oxide grain population be mainly from $<1.5M_{\odot}$ stars. According to the FRANEC models such stars of solar metallicity never become C-rich because the number of thermal pulses is small and not enough ^{12}C is mixed into the envelope by TDU. In this case, the oxides could have, on average, higher $^{26}\text{Al}/^{27}\text{Al}$ ratios than the SiC grains, since the predicted $^{26}\text{Al}/^{27}\text{Al}$ ratios decrease with increasing mass (Fig. 7). However, the predicted ratios are much too small to explain the oxide data.

Thus, CBP probably plays an important role. The $^{26}\text{Al}/^{27}\text{Al}$ ratios observed in SiC grains from AGB stars can be satisfactorily explained by AGB models that involve only ^{26}Al production in the H-burning shell and mixing into the envelope by subsequent TDU episodes. In contrast, the $^{26}\text{Al}/^{27}\text{Al}$ ratios in a substantial number of oxide grains require CBP. We have already mentioned the possibility that CBP prevents stars that experience it from becoming carbon stars and the Nollett et al. (2003) model predicts this to be the case for high circulation rates (see their Figs. 9 and 10). Such stars could thus produce oxide grains with high $^{26}\text{Al}/^{27}\text{Al}$ ratios but, since they do not become C-rich, never produce SiC grains. Stellar rotation is a strong contender for causing CBP, at least in stars on the RGB (Zahn, 1992; Charbonnel, 2004). Since stars have a range of rotation rates it is not inconceivable that those with higher rotation rates experience CBP whereas those with low rotation rates do not and become carbon stars. The O isotopic data indicate that a majority of the spinel grains of groups 1 and 3, although not those with the highest $^{26}\text{Al}/^{27}\text{Al}$ ratios, have inferred parent star masses of less than $1.5M_{\odot}$. According to our AGB models, stars with such low masses and solar metallicity and Reimers' parameter $\eta \geq 0.3$ never become carbon stars and stars with $<1.2M_{\odot}$ are not predicted to become carbon stars, regardless of the value of Reimers' parameter. These stars have a lower temperature in the convective thermal pulse, so that ^{26}Al , produced in the H burning shell and brought into the He intershell, is not strongly depleted by neutron captures. In addition, the mass of the H-burning shell is larger than in more massive AGB stars. The envelope mass is quite low too, thus a few TDU episodes are sufficient to make the envelope ^{26}Al -rich, with $^{26}\text{Al}/^{27}\text{Al}$ up to ~ 0.005 . At this point we can only speculate, but it is clear that the $^{26}\text{Al}/^{27}\text{Al}$ ratios inferred from isotopic analysis of presolar oxide and SiC grains tell us something important about the evolution of AGB stars.

4.7. Chromium Isotopes

With the exception of moderate ^{54}Cr depletions in grains OR1 and OR4, the Cr isotopic ratios of the two Cr-rich spinel

grains and two measured Al-Mg spinel grains are solar within errors (Table 2). Let us consider theoretical expectations for how the GCE and nucleosynthetic processes discussed above should affect Cr isotopes. The Cr isotopes are not affected at all by H burning, but neutron capture reactions in the He-shell of AGB stars can cause slight depletions in ^{50}Cr and excesses of ^{54}Cr in the envelope while the $^{53}\text{Cr}/^{52}\text{Cr}$ ratio remains essentially unchanged. For example, we find in a solar-metallicity $2M_{\odot}$ star that compositional changes in the stellar envelope range from $\delta^{50}\text{Cr}/^{52}\text{Cr} = -12$ to -20 , $\delta^{53}\text{Cr}/^{52}\text{Cr} = 0$ and $\delta^{54}\text{Cr}/^{52}\text{Cr} = 32$ to 80% from the time the star becomes a carbon star to the last TDU episode. For a $5M_{\odot}$ star these ranges are $\delta^{50}\text{Cr}/^{52}\text{Cr} = -4$ to -9 , $\delta^{53}\text{Cr}/^{52}\text{Cr} = 0$ and $\delta^{54}\text{Cr}/^{52}\text{Cr} = 148$ to 444% . It was suggested above that the highly ^{25}Mg and ^{26}Mg enriched grain OC2 might have originated in an intermediate mass star undergoing HBB. Its measured $\delta^{54}\text{Cr}/^{52}\text{Cr}$ value of $102 \pm 116\%$ is consistent with the prediction for a $5M_{\odot}$ AGB star with $\text{C} < \text{O}$, but the large error bar limits the usefulness of the comparison. Since the other grains are believed to have originated in low-mass stars, based on their O isotopic ratios, their Cr isotopic compositions are not expected to be significantly affected by nucleosynthesis in their parent stars, i.e., the predicted shifts in $\delta^{54}\text{Cr}$ are smaller than the experimental uncertainties.

As we have seen for O and Mg, initial compositions of stars are expected to have variations in Cr isotopic composition due to GCE. The Cr isotopes are made in nature by various processes in both Type Ia (Woosley and Weaver, 1994; Nomoto et al., 1997; Woosley, 1997) and Type II supernovae (Woosley and Weaver, 1995) and the GCE model of Timmes et al. (1995) predicts that $^{50,53,54}\text{Cr}/^{52}\text{Cr}$ all increase with increasing metallicity in the Galactic disk (F. Timmes, pers. comm.). For example, a $0.9Z_{\odot}$ star is predicted to have $\delta^{50}\text{Cr}$, $\delta^{53}\text{Cr}$, and $\delta^{54}\text{Cr}$ values of $\sim -150\%$, -100% , and -150% , respectively. The $\sim 10\%$ depletions in ^{54}Cr observed in two grains might thus suggest an origin in stars of slightly lower than solar metallicity. However, if this is the case, the expected accompanying depletions in ^{50}Cr are not observed in the grains. Type II and Ia supernovae are not able to produce the solar abundance of ^{54}Cr . This neutron-rich isotope, together with ^{48}Ca , ^{50}Ti and some of ^{58}Fe is believed to be produced by deflagrations of near Chandrasekhar-mass white dwarf stars (Meyer et al., 1996; Woosley, 1997). Because such events likely comprise only $\sim 2\%$ of all Type Ia explosions, it is expected that ^{54}Cr is very heterogeneously distributed in the interstellar medium and anomalies in ^{54}Cr might reflect this fact.

5. CONCLUSIONS

By measuring the O isotopic compositions of submicron grains in acid residues we have identified 30 presolar spinel grains and measured their Mg isotopic ratios. Two of the grains are Cr-rich with approximate chemical formula MgCrAlO_4 . The O isotopic ratios of the grains fall into all four previously defined groups and indicate that most of the grains come from RGB or AGB stars. The grains have excesses and deficits in ^{25}Mg and several of them have large ^{26}Mg excesses, most likely from the decay of ^{26}Al . Comparison with models of nucleosynthesis in TP-AGB stars show that inferred $^{26}\text{Al}/^{27}\text{Al}$ ratios are much larger than predicted for H-shell production and third dredge-up and imply an extra pro-

duction process of ^{26}Al , most likely cool bottom processing. On average, $^{26}\text{Al}/^{27}\text{Al}$ ratios in oxide grains are larger than those in SiC grains from AGB stars, indicating that stars producing these classes of grains differed from one another in some fundamental way. A possibility is that the parent stars of the oxide grains with high $^{26}\text{Al}/^{27}\text{Al}$ ratios underwent CBP that prevented these stars from becoming carbon stars so that stars with CBP did not produce any presolar SiC grains. These differences in $^{26}\text{Al}/^{27}\text{Al}$ ratios are evidence that presolar oxide grains originated in O-rich stars.

Acknowledgments—This paper is dedicated to the memory of Bob Walker. His leadership and boundless enthusiasm for science made the “fourth floor laboratory” a special place for research and will never be forgotten. His efforts were instrumental in the establishment of the NanoSIMS at Washington University, which played an important role in the work reported here. We thank Tang Ming for producing the Murray residue, Roy Lewis for providing samples and a critical reading of the manuscript, Joachim Huth for taking SEM images, and Sachiko Amari, Tom Bernatowicz, Kuljeet Marhas, Katharina Lodders, and Frank Stadermann for their assistance and for discussions. LRN and EZ thank Günter Lugmair for his hospitality at the MPI for Chemistry in Mainz. Detailed reviews by Andy Davis, Gary Huss and an anonymous reviewer helped in improving the paper and are gratefully acknowledged. This work was supported by NASA Grants NAG5-11545 and NAG5-12917.

Associate editor: M. Grady

REFERENCES

- Alexander C. M. O'D. and Nittler L. R. (1999) The galactic evolution of Si, Ti and O isotopic ratios. *Astrophys. J.* **519**, 222–235.
- Alibés A., Labay J. and Canal R. (2001) Galactic chemical abundance evolution in the solar neighborhood up to the iron peak. *Astron. Astrophys.* **370**, 1103–1121.
- Allende Prieto C., Lambert D. L. and Asplund M. (2001) The forbidden abundance of oxygen in the sun. *Astrophys. J.* **556**, L63–L66.
- Allende Prieto C., Lambert D. L. and Asplund M. A. (2002) reappraisal of the solar photospheric C/O ratio. *Astrophys. J.* **573**, L137–L140.
- Amari S., Hoppe P., Zinner E. and Lewis R. S. (1995) Trace-element concentrations in single circumstellar silicon carbide grains from the Murchison meteorite. *Meteoritics* **30**, 679–693.
- Amari S., Gao X., Nittler L. R., Zinner E., José J., Hernanz M. and Lewis R. S. (2001a) Presolar grains from novae. *Astrophys. J.* **551**, 1065–1072.
- Amari S., Nittler L. R., Zinner E., Gallino R., Lugaro M. and Lewis R. S. (2001b) Presolar SiC grains of type Y: Origin from low-metallicity AGB stars. *Astrophys. J.* **546**, 248–266.
- Amari S., Nittler L. R., Zinner E., Lodders K. and Lewis R. S. (2001c) Presolar SiC grains of type A and B: Their isotopic compositions and stellar origins. *Astrophys. J.* **559**, 463–483.
- Anders E. and Grevesse N. (1989) Abundances of the elements: Meteoritic and solar. *Geochim. Cosmochim. Acta* **53**, 197–214.
- Arndt T. U., Fleischer A. J. and Sedlmayr E. (1997) Circumstellar dust shells around long-period variables VI. An approximative formula for the mass loss rate of C-rich stars. *Astron. Astrophys.* **327**, 614–619.
- Arnould M., Goriely S. and Jorissen A. (1999) Non-explosive hydrogen and helium burnings: Abundance predictions from the NACRE reaction rate compilation. *Astron. Astrophys.* **347**, 572–582.
- Bennett C. L., Halpern M., Hinshaw G., Jarosik N., Kogut A., Limon M., Meyer S. S., Page L., Spergel D. N., Tucker G. S., Wollack E., Wright E. L., Barnes C., Greason M. R., Hill R. S., Komatsu E., Nolte M. R., Odegard N., Peiris H. V., Verde L. and Weiland J. L. (2003) First-Year Wilkinson Microwave Anisotropy Probe (WMAP) observations: Preliminary maps and basic results. *Astrophys. J.* **148**, 1–27.
- Bensby T., Feltzing S. and Lundström I. (2003) Elemental abundance trends in the Galactic thin and thick disks as traced by nearby F and G dwarf stars. *Astron. Astrophys.* **410**, 527–551.
- Bensby T., Feltzing S. and Lundström I. (2004) Oxygen trends in the Galactic thin and thick disks. *Astron. Astrophys.* **415**, 155–170.
- Bernatowicz T. J., Messenger S., Pravdivtseva O., Swan P. and Walker R. M. (2003) Pristine presolar silicon carbide. *Geochim. Cosmochim. Acta* **67**, 4679–4691.
- Boothroyd A. I. and Sackmann I.-J. (1988) Low-mass stars. III. Low-mass stars with steady mass loss: up to the asymptotic giant branch and through the final thermal pulses. *Astrophys. J.* **328**, 653–670.
- Boothroyd A. I. and Sackmann I.-J. (1999) The CNO isotopes: deep circulation in red giants and first and second dredge-up. *Astrophys. J.* **510**, 232–250.
- Boothroyd A. I., Sackmann I.-J. and Wasserburg G. J. (1994) Predictions of oxygen isotope ratios in stars and of oxygen-rich interstellar grains in meteorites. *Astrophys. J.* **430**, L77–L80.
- Boothroyd A. I., Sackmann I.-J. and Wasserburg G. J. (1995) Hot bottom burning in asymptotic giant branch stars and its effect on oxygen isotopic abundances. *Astrophys. J.* **442**, L21–L24.
- Busso M., Gallino R. and Wasserburg G. J. (1999) Nucleosynthesis in asymptotic giant branch stars: relevance for Galactic enrichment and solar system formation. *Ann. Rev. Astron. Astrophys.* **37**, 239–309.
- Charbonnel C. A. (1995) consistent explanation for $^{12}\text{C}/^{13}\text{C}$, ^7Li and ^3He anomalies in red giant stars. *Astrophys. J.* **453**, L41–L44.
- Charbonnel C. (2004) The impact of rotation on chemical abundances in red giant branch stars. In *Carnegie Observatories Astrophysics Series, Origin and Evolution of the Elements* (eds. A. McWilliam and M. Rauch), Vol. 4. pp. 60–67. Cambridge Univ. Press, Cambridge.
- Choi B.-G., Huss G. R., Wasserburg G. J. and Gallino R. (1998) Presolar corundum and spinel in ordinary chondrites: Origins from AGB stars and a supernova. *Science* **282**, 1284–1289.
- Choi B.-G., Wasserburg G. J. and Huss G. R. (1999) Circumstellar hibonite and corundum and nucleosynthesis in asymptotic giant branch stars. *Astrophys. J.* **522**, L133–L136.
- Ebel D. S. (2000) Variations on solar condensation: Sources of interstellar dust nuclei. *J. Geophys. Res.* **105**, 10,363–10,370.
- Fenner Y., Gibson B. K., Lee H.-C., Karakas A. I., Lattanzio J. C., Chieffi A., Limongi M. and Yong D. (2003) The chemical evolution of magnesium isotopic abundances in the solar neighbourhood. *Pub. Astron. Soc. Austr.* **20**, 340–344.
- Forestini M. and Charbonnel C. (1997) Nucleosynthesis of light elements inside thermally pulsing AGB stars: I. The case of intermediate-mass stars. *Astron. Astrophys. Suppl.* **123**, 241–272.
- Forestini M., Paulus G. and Arnould M. (1991) On the production of ^{26}Al in AGB stars. *Astron. Astrophys.* **252**, 597–604.
- Fuhrmann K. (1998) Nearby stars of the Galactic disk and halo. *Astron. Astrophys.* **338**, 161–183.
- Gallino R., Arlandini C., Busso M., Lugaro M., Travaglio C., Straniero O., Chieffi A. and Limongi M. (1998) Evolution and nucleosynthesis in low-mass asymptotic giant branch stars. II. Neutron capture and the s-process. *Astrophys. J.* **497**, 388–403.
- Gallino R., Busso M. and Lugaro M. (1997) Neutron capture nucleosynthesis in AGB stars. In *Astrophysical Implications of the Laboratory Study of Presolar Materials* (eds. T. J. Bernatowicz and E. Zinner), pp. 115–153. AIP, New York.
- Gay P. L. and Lambert D. L. (2000) The isotopic abundances of magnesium in stars. *Astrophys. J.* **533**, 260–270.
- Goswami A. and Prantzos N. (2000) Abundance evolution of intermediate mass elements (C to Zn) in the Milky Way halo and disk. *Astron. Astrophys.* **359**, 191–212.
- Hoppe P., Amari S., Zinner E., Ireland T. and Lewis R. S. (1994) Carbon, nitrogen, magnesium, silicon and titanium isotopic compositions of single interstellar silicon carbide grains from the Murchison carbonaceous chondrite. *Astrophys. J.* **430**, 870–890.
- Hoppe P., Amari S., Zinner E. and Lewis R. S. (1995) Isotopic compositions of C, N, O, Mg, and Si, trace element abundances and morphologies of single circumstellar graphite grains in four density fractions from the Murchison meteorite. *Geochim. Cosmochim. Acta* **59**, 4029–4056.
- Hoppe P., Annen P., Strebel R., Eberhardt P., Gallino R., Lugaro M., Amari S. and Lewis R. S. (1997) Meteoritic silicon carbide grains with unusual Si-isotopic compositions: Evidence for an origin in low-mass metallicity asymptotic giant branch stars. *Astrophys. J.* **487**, L101–L104.

- Hoppe P. and Ott U. (1997) Mainstream silicon carbide grains from meteorites. In *Astrophysical Implications of the Laboratory Study of Presolar Materials* (eds. T. J. Bernatowicz and E. Zinner), pp. 27–58. AIP, New York
- Hoppe P., Strebler R., Eberhardt P., Amari S. and Lewis R. S. (2000) Isotopic properties of silicon carbide X grains from the Murchison meteorite in the size range 0.5–1.5 μm . *Meteorit. Planet. Sci.* **35**, 1157–1176.
- Huss G. R., Fahey A. J. and Wasserburg G. J. (1995) Problems in the nucleosynthesis of O, Mg and Ti in an Al_2O_3 grain from an AGB star. *Lunar Planet. Sci.* **XXVI**, 643–644.
- Huss G. R., Hutcheon I. D. and Wasserburg G. J. (1997) Isotopic systematics of presolar silicon carbide from the Orgueil (CI) carbonaceous chondrite: Implications for solar system formation and stellar nucleosynthesis. *Geochim. Cosmochim. Acta* **61**, 5117–5148.
- Huss G. R., Hutcheon I. D., Wasserburg G. J. and Stone J. (1992) Presolar (?) corundum in the Orgueil meteorite. *Lunar Planet. Sci.* **XXIII**, 563–564.
- Hutcheon I. D., Huss G. R., Fahey A. J. and Wasserburg G. J. (1994) Extreme ^{26}Mg and ^{17}O enrichments in an Orgueil corundum: Identification of a presolar oxide grain. *Astrophys. J.* **425**, L97–L100.
- Karakas A. I. (2003) Asymptotic giant branch stars: their influence on binary systems and the interstellar medium. Ph.D. thesis, Monash University, Australia.
- Karakas A. I. and Lattanzio J. C. (2003) Production of aluminium and the heavy magnesium isotopes in asymptotic giant branch stars. *Pub. Astron. Soc. Austr.* **20**, 279–293.
- Koehler P. E., Kavanagh R. W., Vogelaar R. B., Glendenov Y. M. and Popov Y. P. (1997) $^{26}\text{Al}(n,p_1)$ and (n,α_0) cross sections from thermal energy to 70 keV and the nucleosynthesis of ^{26}Al . *Phys. Rev. C* **56**, 1138–1143.
- Krauss L. M. and Chaboyer B. (2003) Age estimates of globular clusters in the Milky Way: Constraints on cosmology. *Science* **299**, 65–70.
- Krestina N., Hsu W. and Wasserburg G. J. (2002) Circumstellar oxide grains in ordinary chondrites and their origin. *Lunar Planet. Sci.* **XXXIII**, Abstract #1425.
- Lampens P., Kovalevsky J., Froeschlé M. and Ruymaekers G. (1997) On the mass-luminosity relation. *Proceedings of the ESA Symposium "Hipparcos—Venice '97"* **ESA SP-402**, 421–424.
- Larimer J. W. and Bartholomay M. (1979) The role of carbon and oxygen in cosmic gases: some applications to the chemistry and mineralogy of enstatite chondrites. *Geochim. Cosmochim. Acta* **43**, 1455–1466.
- Lattanzio J., Forestini M. and Charbonnel C. (2000) Nucleosynthesis in intermediate mass AGB stars. *Mem. Soc. Astron. It.* **71**, 737–744.
- Lattanzio J., Frost C., Cannon R. and Wood P. (1996) Hot bottom burning in intermediate mass stars. *Mem. Soc. Astro. It.* **67**, 729–748.
- Lattanzio J. C., Frost C. A., Cannon R. C. and Wood P. R. (1997) Hot bottom burning nucleosynthesis in $6M_{\odot}$ stellar models. *Nuclear Physics A* **621**, 435c–438c.
- Lodders K. and Fegley B., Jr. (1995) The origin of circumstellar silicon carbide grains found in meteorites. *Meteoritics* **30**, 661–678.
- Lugaro M., Davis A. M., Gallino R., Pellin M. J., Straniero O. and Käppeler F. (2003) Isotopic compositions of strontium, zirconium, molybdenum and barium in single presolar SiC grains and asymptotic giant branch stars. *Astrophys. J.* **593**, 486–508.
- Lugaro M., Zinner E., Gallino R. and Amari S. (1999) Si isotopic ratios in mainstream presolar SiC grains revisited. *Astrophys. J.* **527**, 369–394.
- Marhas K. K., Hoppe P. and Bismehn A. (2004) A NanoSIMS study of iron-isotopic compositions in presolar silicon carbide grains. *Lunar Planet. Sci.* **XXXV**, Abstract #1834.
- Martin C., Mignard F., Hartkopf W. I. and McAlister H. A. (1998) Mass determination of astrometric binaries with Hipparcos. III. New results for 28 systems *Astron. Astrophys.* **133**, 149–162.
- McWilliam A. (1997) Abundance ratios and galactic chemical evolution. *Ann. Rev. Astron. Astrophys.* **35**, 503–556.
- McWilliam A. and Lambert D. L. (1988) Isotopic magnesium abundances in stars. *Mon. Not. R. Astr. Soc.* **230**, 573–585.
- Meyer B. S., Krishnan T. D. and Clayton D. D. (1996) ^{48}Ca production in matter expanding from high temperature and density. *Astrophys. J.* **462**, 825–838.
- Mowlavi N. and Meynet G. (2000) Aluminum 26 production in asymptotic giant branch stars. *Astron. Astrophys.* **361**, 959–976.
- Nguyen A., Zinner E. and Lewis R. S. (2003) Identification of small presolar spinel and corundum grains by isotopic raster imaging. *Publ. Astron. Soc. Austr.* **20**, 382–388.
- Nittler L. R. (1997) Presolar oxide grains in meteorites. In *Astrophysical Implications of the Laboratory Study of Presolar Materials* (eds. T. J. Bernatowicz and E. Zinner), pp. 59–82. AIP, New York.
- Nittler L. R. (2003) Presolar stardust in meteorites: recent advances and scientific frontiers. *Earth Planet. Sci. Lett.* **209**, 259–273.
- Nittler L. R. (2005) Constraints on heterogeneous galactic chemical evolution from meteoritic stardust. *Astrophys. J.* **618**, 281–296.
- Nittler L. R. and Alexander C. M. O'D. (1999) Automatic identification of presolar Al- and Ti-rich oxide grains from ordinary chondrites. *Lunar Planet. Sci.* **XXX**, Abstract #2041.
- Nittler L. R. and Alexander C. M. O'D. (2003a) Automated isotopic measurements of micron-sized dust: Application to meteoritic presolar silicon carbide. *Geochim. Cosmochim. Acta* **67**, 4961–4980.
- Nittler L. R. and Alexander C. M. O'D. (2003b) Chromium-bearing presolar oxide grains in a ^{54}Cr -rich Orgueil residue. *Meteorit. Planet. Sci.* **38**, A129.
- Nittler L. R., Alexander C. M. O'D., Gao X., Walker R. M. and Zinner E. (1997) Stellar sapphires: The properties and origins of presolar Al_2O_3 in meteorites. *Astrophys. J.* **483**, 475–495.
- Nittler L. R., Alexander C. M. O'D., Gao X., Walker R. M. and Zinner E. K. (1994) Interstellar oxide grains from the Tieschitz ordinary chondrite. *Nature* **370**, 443–446.
- Nittler L. R., Alexander C. M. O'D., Stadermann F. J., and Zinner E. K. (2005) Presolar Al-, Ca- and Ti-rich oxide grains in the Krymka meteorite. *Lunar Planet. Sci.* **XXXVI**, Abstract #2200.
- Nittler L. R., Hoppe P., Alexander C. M. O'D., Amari S., Eberhardt P., Gao X., Lewis R. S., Strebler R., Walker R. M. and Zinner E. (1995) Silicon nitride from supernovae. *Astrophys. J.* **453**, L25–L28.
- Nittler L. R., Hoppe P., Alexander C. M. O'D., Busso M., Gallino R., Marhas K. K. and Nollett K. (2003) Magnesium isotopes in presolar spinel. *Lunar Planet. Sci.* **XXXIV**, Abstract #1703.
- Nollett K. M., Busso M. and Wasserburg G. J. (2003) Cool bottom processes on the thermally pulsing asymptotic giant branch and the isotopic composition of circumstellar dust grains. *Astrophys. J.* **582**, 1036–1058.
- Nomoto K., Iwamoto K., Nakasato N., Thielemann F.-K., Brachwitz F., Tsujimoto T., Kubo Y. and Kishimoto N. (1997) Nucleosynthesis in type IA supernovae. *Nuclear Phys. A* **621**, 467c–476c.
- Prantzos N., Aubert O. and Audouze J. (1996) Evolution of the carbon and oxygen isotopes in the Galaxy. *Astron. Astrophys.* **309**, 760–774.
- Reddy B. E., Tomkin J., Lambert D. L. and Allende Prieto C. (2003) The chemical compositions of Galactic disk F and G dwarfs. *Mon. Not. R. Astron. Soc.* **340**, 304–340.
- Reimers D. (1975) Circumstellar envelopes and mass loss of red giant stars. In *Problems in stellar atmospheres and envelopes* (eds. B. Baschek, W. H. Kegel and G. Traving), pp. 229–256. Springer-Verlag, New York.
- Scalo J. M. (1986) The stellar initial mass function. *Fundam. Cosm. Phys.* **11**, 1–278.
- Simon S. B., Yoneda S., Grossman L. and Davis A. M. (1994) A CaAl_2O_7 -bearing refractory spherule from Murchison—Evidence for very high-temperature melting in the solar nebula. *Geochim. Cosmochim. Acta* **58**, 1937–1949.
- Sloan G. C., Kraemer K. E., Goebel J. H. and Price S. D. (2003) Guilt by association: The 13 micron dust emission feature and its correlation to other gas and dust features. *Astrophys. J.* **594**, 483–495.
- Slodzian G., Hillion F., Stadermann F. J. and Horreard F. (2003) Oxygen isotopic measurements on the CAMECA NanoSIMS 50. *Appl. Surf. Sci.* **203–204**, 798–801.
- Speck A. K., Barlow M. J., Sylvester R. J. and Hofmeister A. M. (2000) Dust features in the 10- μm infrared spectra of oxygen-rich evolved stars. *Astron. Astrophys. Suppl.* **146**, 437–464.

- Straniero O., Chieffi A., Limongi M., Busso M., Gallino R. and Arlandini C. (1997) Evolution and nucleosynthesis in low-mass asymptotic giant branch stars. I. Formation of population I carbon stars *Astrophys. J.* **478**, 332–339.
- Straniero O., Domínguez I., Cristallo S. and Gallino R. (2003) Low-mass AGB stellar models for $0.003 \leq Z \leq 0.02$: Basic formulae for nucleosynthesis calculations. *Publ. Astron. Soc. Austr.* **20**, 389–392.
- Straniero O., Gallino R. and Cristallo S. (2005) s Process in low-mass asymptotic giant branch stars. *Nucl. Phys. A* in press.
- Tang M. and Anders E. (1988) Isotopic anomalies of Ne, Xe and C in meteorites. II. Interstellar diamond and SiC: Carriers of exotic noble gases. *Geochim. Cosmochim. Acta* **52**, 1235–1244.
- Timmes F. X., Woosley S. E. and Weaver T. A. (1995) Galactic chemical evolution: Hydrogen through zinc. *Astrophys. J. Suppl.* **98**, 617–658.
- Travaglio C., Gallino R., Amari S., Zinner E., Woosley S. and Lewis R. S. (1999) Low-density graphite grains and mixing in type II supernovae. *Astrophys. J.* **510**, 325–354.
- Wasserburg G. J., Boothroyd A. I. and Sackmann I.-J. (1995) Deep circulation in red giant stars: A solution to the carbon and oxygen isotope puzzles? *Astrophys. J.* **447**, L37–L40.
- Wood J. A. and Hashimoto A. (1993) Mineral equilibrium in fractionated nebular systems. *Geochim. Cosmochim. Acta* **57**, 2377–2388.
- Woosley S. E. (1997) Neutron-rich nucleosynthesis in carbon deflagration supernovae. *Astrophys. J.* **476**, 801–810.
- Woosley S. E. and Weaver T. A. (1994) Sub-chandrasekhar mass models for type Ia supernovae. *Astrophys. J.* **423**, 371–379.
- Woosley S. E. and Weaver T. A. (1995) The evolution and explosion of massive stars. II. Explosive hydrodynamics and nucleosynthesis *Astrophys. J. Suppl.* **101**, 181–235.
- Yong D., Lambert D. L. and Ivans I. I. (2003) Magnesium isotopic abundance ratios in cool stars. *Astrophys. J.* **599**, 1357–1371.
- Zahn J.-P. (1992) Circulation and turbulence in rotating stars. *Astron. Astrophys.* **265**, 115–132.
- Zinner E. (2003) Presolar grains. In *Meteorites, Planets and Comets* (ed. A. M. Davis), Vol. 1, *Treatise on Geochemistry* (eds. H. D. Holland and K. K. Turekian), pp. 17–39. Elsevier-Pergamon, Oxford.
- Zinner E., Amari S., Anders E. and Lewis R. S. (1991) Large amounts of extinct ^{26}Al in interstellar grains from the Murchison carbonaceous chondrite. *Nature* **349**, 51–54.
- Zinner E., Amari S., Guinness R., Nguyen A., Stadermann F., Walker R. M. and Lewis R. S. (2003) Presolar spinel grains from the Murray and Murchison carbonaceous chondrites. *Geochim. Cosmochim. Acta* **67**, 5083–5095.
- Zinner E., Amari S., Jennings C., Mertz A. F., Nguyen A. N., Nittler L. R., Hoppe P., Gallino R. and Lugaro M. (2005) Al and Ti isotopic ratios of presolar SiC grains of type Z. *Lunar Planet. Sci.* **XXXVI**, Abstract #1691.
- Zinner E., Nittler L. R., Hoppe P., Gallino R. and Lewis R. S. (2004) Oxygen and magnesium isotopic ratios of presolar spinel grains. *Lunar Planet. Sci.* **XXXV**, Abstract #1337.